JOURNAL OF PETROLOGY | VOLUME 47 | NUMBER 8 | PAGES 1611–1636 | 2006 | doi:10.1093/petrology/egl022

Transformation of Archaean Lithospheric Mantle by Refertilization: Evidence from Exposed Peridotites in the Western Gneiss Region, Norway

ELOISE E. BEYER[1]*, WILLIAM L. GRIFFIN[1,2] AND SUZANNE Y. O'REILLY[1]

[1]ARC NATIONAL KEY CENTRE FOR GEOCHEMICAL EVOLUTION AND METALLOGENY OF CONTINENTS, DEPARTMENT OF EARTH AND PLANETARY SCIENCES, MACQUARIE UNIVERSITY, NSW 2109, AUSTRALIA

[2]CSIRO EXPLORATION AND MINING, NORTH RYDE, NSW 2113, AUSTRALIA

RECEIVED AUGUST 25, 2005; ACCEPTED MARCH 24, 2006; ADVANCE ACCESS PUBLICATION APRIL 28, 2006

Orogenic peridotites occur enclosed in Proterozoic gneisses at several localities in the Western Gneiss Region (WGR) of western Norway; garnet peridotites typically occur as discrete zones within larger bodies of garnet-free, chromite-bearing dunite and are commonly closely associated with pyroxenites and eclogites. The dunites of the large Almklovdalen peridotite body have extremely depleted compositions (Mg-number 92–93·6); the garnet peridotites have lower Mg-number (90·6–91·7) and higher whole-rock Ca and Al contents. Post-depletion metasomatism of both rock types is indicated by variable enrichment in the light rare earth elements, Th, Ba and Sr. The dunites can be modelled as residues after very high degrees (>60%) of melt extraction at high pressure (5–7 GPa), inconsistent with the preservation of lower degrees of melting in the garnet peridotites. The garnet peridotites are, therefore, interpreted as zones of melt percolation, which resulted in refertilization of the dunites by a silicate melt rich in Fe, Ca, Al and Na, but not Ti. Previous Re–Os dating gives Archaean model ages for the dunites, but mixed Archaean and Proterozoic ages for the garnet peridotites, suggesting that refertilization occurred in Proterozoic time. At least some Proterozoic lithosphere may represent reworked and transformed Archaean lithospheric mantle.

KEY WORDS: *Archaean mantle; Proterozoic mantle; Western Gneiss Region, Norway; mantle metasomatism; garnet peridotite*

INTRODUCTION

Peridotite bodies occur within many high-pressure (HP) and ultrahigh-pressure (UHP) metamorphic terranes in the root-zones of mountain belts formed by continental collision (e.g. Brueckner & Medaris, 2000). Variously called 'orogenic peridotites', 'peridotite massifs' and 'alpine-type peridotites', they typically occur within metamorphosed continental crustal rocks as lensoid masses that range in outcrop dimensions from $1\,m^2$ to $>100\,km^2$.

These tectonically emplaced peridotite complexes provide the opportunity to interpret large-scale mantle structures and rock-type relationships, and are an important complement to the relatively small samples provided as mantle xenoliths brought to the Earth's surface in a range of volcanic rocks. Although xenoliths globally sample a greater geographical and depth range of the lithospheric mantle than the tectonically emplaced massifs, relationships between rock types are rarely observable. Studies of the spatial and structural relationships of rock types that crop out in orogenic peridotites, combined with detailed geochemical analysis, allow a fuller understanding of processes important to the evolution of the lithospheric mantle and improve our ability to interpret the xenolith data.

*Corresponding author. E-mail: ebeyer@els.mq.edu.au

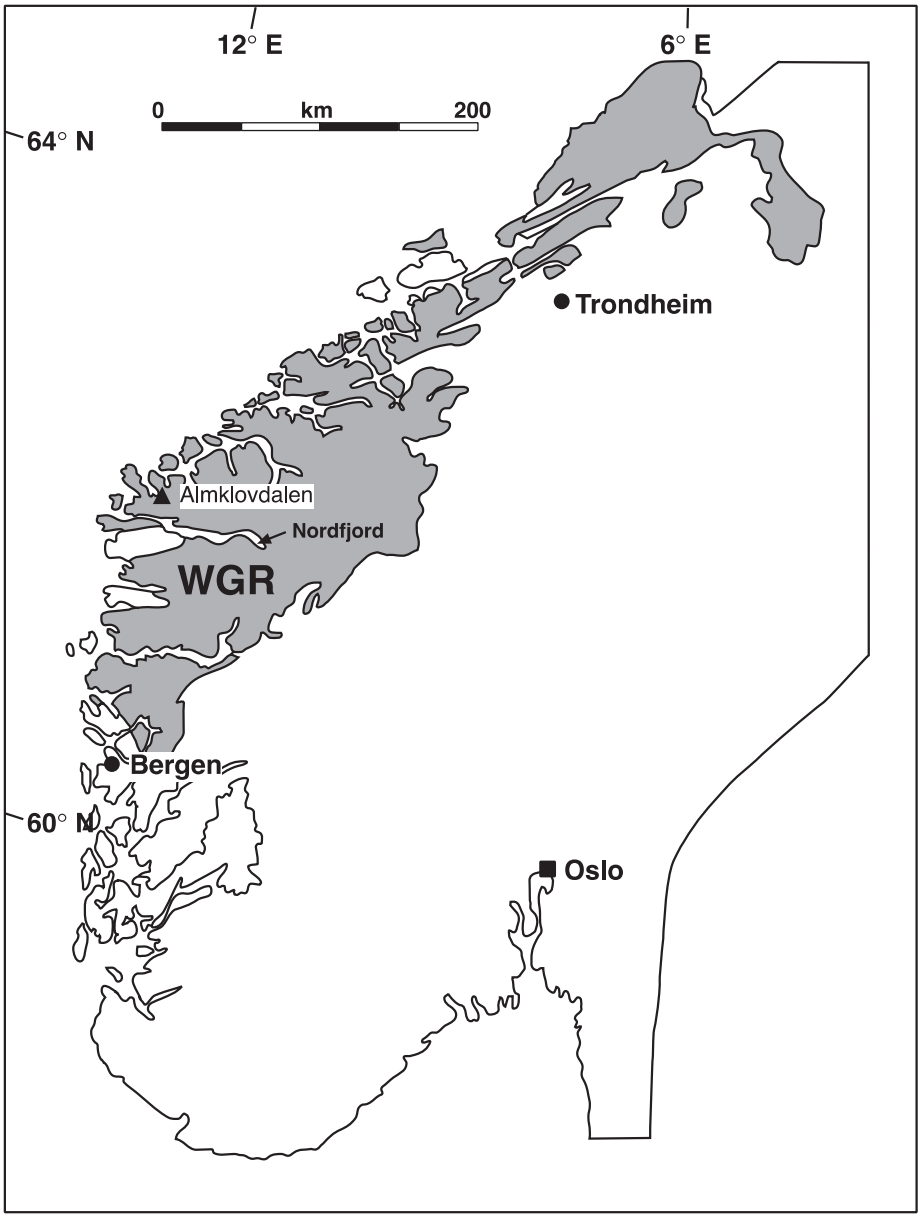

Fig. 1. Map of the Western Gneiss Region (WGR), Norway. Modified after Cuthbert *et al.* (1983).

Recent studies of orogenic massifs have revealed a diversity of rock types similar in composition and mineralogy to some kimberlite- and basalt-borne mantle xenoliths. Most massif peridotites are spinel-bearing but garnet-bearing examples are widespread. Garnet-bearing rock types include lherzolite, harzburgite, wehrlite, dunite and pyroxenite, and most examples have been recrystallized to varying degrees, resulting in lower-pressure anhydrous and hydrous mineral assemblages (e.g. Brueckner & Medaris, 2000).

Garnet peridotites are widely distributed across the Western Gneiss Region (WGR) of western Norway (Fig. 1) and typically occur as small volumes within larger bodies of olivine–orthopyroxene rocks, collectively described in the literature as 'dunite'. Previous work on the Western Gneiss Region peridotites has focused strongly on the garnet peridotites, generally neglecting the volumetrically dominant dunite component (some relevant references include Bryhni, 1966; Lappin, 1966, 1974; O'Hara, 1967; Carswell, 1968*a*, 1968*b*, 1974; Bryhni *et al.*, 1969; Bryhni & Green, 1970; O'Hara *et al.*, 1971; Green & Mysen, 1972; Griffin & Råheim, 1973; Lappin & Smith, 1978). These dunites have long been considered to represent retrograded garnet peridotites,

based on the close spatial relationship between the two rock types and evidence for retrogression of garnet to chlorite along the margins of the garnet peridotite bodies (e.g. Medaris, 1980, 1984; Griffin & Qvale, 1985). However, as shown in this study, most dunites, at least at the large Almklovdalen body in the southern part of the Western Gneiss Region, are highly refractory (i.e. are strongly depleted in basaltic components) and, therefore, cannot represent retrograded garnet peridotite. This observation has important implications for the genesis of the garnet-bearing rocks and their relationship to their host dunites.

More recent papers on the WGR have focused on contrast and comparison with other Eurasian peridotite massifs (Medaris & Carswell, 1990; Ernst *et al.*, 1995; Krogh & Carswell, 1995; Brueckner & Medaris, 1998; Carswell *et al.*, 1999; Medaris, 1999). In the light of geochemical, geothermobarometric and geochronological data it is now widely accepted that the garnet peridotite bodies in the WGR are unique and represent a rare example of ancient subcontinental lithosphere that has been tectonically emplaced into the crust with its upper mantle assemblages largely intact (Medaris, 1999; Brueckner & Medaris, 2000).

In this study, whole-rock major- and trace-element analyses have been performed on the two main mantle-derived rock types, garnet lherzolite and garnet-free dunite, from several localities within the Almklovdalen peridotite body. The geochemical data are used to interpret the history of the peridotites and to examine possible genetic links between the garnet-rich lherzolites and the dunites. *In situ* analysis of the trace-element contents of minerals by laser-ablation ICPMS microprobe, and major element analysis by electron microprobe, have been used to explore the geochemistry of minerals in the peridotites and to understand the processes of partial melting and metasomatism of the lithospheric mantle. Previous results of Re–Os isotopic dating of whole rocks, and of sulphide grains *in situ*, have been integrated with these geochemical data to provide a geochronological framework.

GEOLOGICAL SETTING

The Western Gneiss Region is an elongate area, 300 km long and 150 km wide, stretching along the western coast of Norway from Bergen in the south to Trondheim in the north (Cuthbert *et al.*, 2000; Fig. 1). It includes an assembly of thrust sheets emplaced onto the Baltoscandian continental margin during the final phase of the Caledonian orogeny (Coleman & Wang, 1995). As well as an autochthonous or parautochthonous crystalline basement of Middle Proterozoic or older age, the WGR contains interfolded nappes that have been divided into two principal lithotectonic units: (1) the HP/UHP (high pressure/ultrahigh pressure) metamorphosed Fjordane complex, a mixed assembly of gneiss, supracrustal rocks, anorthosites, augen gneisses and eclogites, exposed to the north and west; (2) the Jøstedal complex, a more monotonous migmatitic orthogneiss unit to the east (Griffin *et al.*, 1985; Ernst *et al.*, 1995). High-pressure rocks such as eclogites and garnet-bearing peridotites are relatively common throughout the WGR, particularly within the western part of the Fjordane Complex [see review by Carswell *et al.* (1999)].

There are hundreds of peridotite bodies in the WGR, some of which are interpreted to be recrystallized from garnet-bearing assemblages to lower-grade assemblages during the Caledonian orogeny (Griffin *et al.*, 1985). Locally, small volumes of relict garnet peridotites and associated garnet pyroxenites and eclogites have been preserved; many of these are totally enclosed within dunite or harzburgite. In addition to garnet lherzolites there are also garnet-bearing harzburgites and dunites, and these rock types may be interlayered at centimetre to metre scales. On a local scale, garnet peridotites commonly surround dyke-like bodies of garnet-bearing websterite, wehrlite, eclogite and clinopyroxenite, indicating one or more periods of melt intrusion while the peridotites were still in the mantle (Medaris, 1980, 1984; Brueckner & Medaris, 1998). Phlogopite and kaersutitic amphibole are associated with some garnet-bearing assemblages, suggesting hydrous metasomatism in the mantle (Brueckner & Medaris, 1998).

The mantle-derived peridotite bodies in the WGR have had a long, complex tectonothermal history with up to eight different metamorphic stages now recognized (Carswell & van Roermund, 2003), many of which are recorded in the Almklovdalen peridotite. The two most prominent mineral assemblages in the Almklovdalen body are olivine + low-Al enstatite + Cr-diopside + pyrope-rich garnet [Stage 2, garnet peridotite; equivalent to Stage II of Carswell (1986)] and olivine + low-Al enstatite + chlorite + tremolite [Stage 7, chlorite-poor dunite; equivalent to Stage VI of Carswell (1986)]. Despite this protracted metamorphic history the peridotites in the WGR are still thought to have been emplaced in the crust with their mantle assemblages largely intact (see discussion above) and these rocks can, therefore, be considered to be representative of the mantle section from which they were derived. It is also worth noting here that many well-documented mantle xenolith suites record similarly complex histories.

The Almklovdalen peridotite body is located ~10 km north of Nordfjord in the southern WGR (Fig. 1) within the zone subjected to UHP metamorphism during Caledonian time [see review by Carswell *et al.* (1999)]. It consists of several large ultramafic outcrops that are inferred to be connected subsurface, forming a

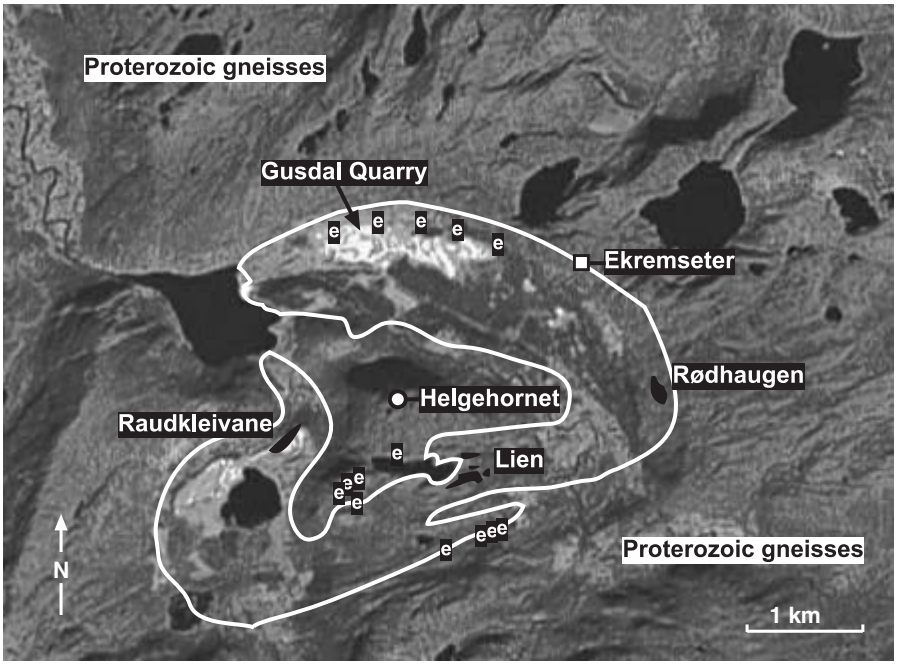

Fig. 2. Map of the Almklovdalen peridotite body showing sample localities. Modified after Griffin & Mørk (1981). Eclogite outcrops denoted by 'e' Satellite image taken from http://maps.google.com/.

bowl-shaped sheet around a central gneiss region (Grønlie & Rost, 1974). A detailed structural study was presented by Cordellier *et al.* (1981). The dominant rock type of the Almklovdalen body is chlorite-poor dunite or harzburgite, which is extensively mined for refractory material by A/S Olivin (the company estimates that approximately two billion tons of high-quality olivine are still available, giving some indication of the immense volume of dunite present in this peridotite body). At three localities (Lien, Raudkleivane and Rødhaugen; see Fig. 2) these highly depleted rocks enclose volumes of chlorite-rich peridotite, which in turn contain small relics of garnet lherzolite, interlayered on a scale of centimetres to metres with wehrlites, low-Na garnet clinopyroxenites and websterites, and less common eclogites. All of these rock types are isoclinally folded together. Retrogression of garnet peridotite to amphibole–chlorite peridotite is evident along the margins of the garnet peridotite bodies, where garnet has been replaced by chlorite and a penetrative foliation, characteristic of the retrograded peridotites, has begun to develop in the garnet peridotite (Medaris, 1980, 1984).

Detailed studies (Medaris, 1980) of the Lien (Helgehornsvatn) locality (Fig. 2) showed that chlorite peridotite is the dominant rock type, and is clearly derived by retrograde metamorphism of garnet peridotite. It is interlayered on all scales with chlorite-poor 'dunite' interpreted as originally garnet-poor dunite–harzburgite. It also contains layers of clinopyroxenite ± garnet, which differ only in modal composition from the relic garnet wehrlites and garnet lherzolites. The structural style in both the surrounding gneisses and the ultramafic–mafic complex is characterized by tight to isoclinal similar folds with penetrative axial-plane foliation; all linear elements are parallel in the peridotites and the host gneisses, and both rock types share all structural elements. Similar observations have been made elsewhere in the WGR (e.g. Brueckner, 1977).

In the Raudkleivane locality (Fig. 2), garnet lherzolite, garnet websterite and garnet clinopyroxenite, interlayered and isoclinally folded on a scale of decimetres to centimetres (Lappin, 1966; see detailed map in the study by Griffin & Qvale, 1985) occur as relics within a body of chlorite peridotite. One outcrop indicates that open folding had occurred prior to the dominant penetrative isoclinal folding. Lappin (1973, 1974) described exsolution features in two of the garnet pyroxenite pods, indicating that they formed by cooling of high-T clinopyroxene cumulates. Fe-rich eclogite bodies, in contrast, show evidence of prograde metamorphism from amphibolites, and are interpreted as boudins of basaltic dykes (Griffin & Qvale, 1985), The zone of chlorite peridotite is only 50–60 m wide across strike, and has sharp foliation-parallel contacts to the enclosing chlorite-poor dunite. The latter rock type has now been mined up to the edge of the chlorite peridotite outcrop, providing fresh samples for this study.

The classic Rødhaugen locality is an isolated knob, in which a metre-thick layer of garnet clinopyroxenite [the 'Rødhaug type eclogite' of Eskola (1921)] defines a

large open fold in garnetiferous peridotite of widely varying mineralogy and degree of retrogression (Carswell, 1981). Contact relationships to the surrounding dunite are not exposed. Rock and mineral analyses have been given by Eskola (1921), O'Hara & Mercy (1963) and Mercy & O'Hara (1965*a*, 1965*b*). The Ekremseter quarry was the first commercial dunite quarry in Almklovdalen; the rock is a dunite with minor orthopyroxene and locally abundant chromite. Large (10–20 cm) ovoid olivine augen occur locally, within a weakly foliated matrix of fresh olivine.

It is clear from the available mapping, and the extensive mining activities (Fig. 2) that the known localities of garnet peridotite or chlorite peridotite are volumetrically minor compared with the chlorite-poor dunite or harzburgite. The known field relationships demonstrate a consistent spatial relationship between the garnet-bearing peridotites (and their retrograded equivalents, the chlorite peridotites) and mafic rocks ranging from clinopyroxenite ± garnet through websterite ± garnet to eclogite. To our knowledge there are no examples of such mafic rocks enclosed in the volumetrically dominant dunite or harzburgite. These relationships raise the question of the genetic relationships between the dunite or harzburgite on the one hand, and the garnet-bearing peridotites on the other.

SAMPLES

Eighteen peridotite samples were selected for study: six garnet lherzolites and 12 dunites. These rocks were collected from three sites, Raudkleivane, Helgehornsvatn and Ekremseter (Fig. 2), and were sampled to cover the range of peridotitic rock types. An additional major-element dataset for nine dunites from the mines in the northern part of the Almklovdalen body (Osland, 1997) was provided by Hannes Brueckner. Two composite 'mine run' dunites (ST89 and ST95), from two quarries in Almklovdalen, were provided by A/S Olivin and were analysed at the GEMOC Geochemical Analysis Unit; they are similar to a 1957–1959 mine-run sample from the Gusdal quarry (Lappin, 1974). To complement this dataset we have also included previously published data for both the dunites and garnet peridotites plus four unpublished dunite analyses by Røst (personal communication, 1975). The pyroxene-rich rocks have been the subject of numerous other studies, and data from those are presented here also.

PETROGRAPHY

Garnet lherzolite

The garnet lherzolites are dominantly porphyroclastic and moderately serpentinized (Fig. 3a). They are characterized by large garnet and pyroxene porphyroclasts in a fine-grained (average grain size <0·5 mm) matrix of recrystallized olivine and pyroxene. Garnet porphyroclasts range in diameter from 2 mm to 1 cm; they are commonly rounded, although more irregular and elongated garnets were also noted. Kelyphite rims on garnets are variably developed and range from 0·1–1·5 mm thick. Partial collars of coarse-grained amphibole and spinel mantle the reaction rims and were interpreted by Carswell (1968*b*) as due to recrystallization of kelyphite. The orthopyroxene porphyroclasts (>4 mm in diameter) are strained; they display strong undulose extinction and, in some instances, kink-banding. Clinopyroxene is apple green and typically occurs as unstrained, equant grains 0·75–2·5 mm across. Serpentine veins crosscut porphyroclasts, including kelyphite rims and amphibole collars on garnet; serpentinization therefore postdates formation and recrystallization of the reaction coronas (Carswell, 1968*b*).

Dunite

The dunites have the assemblage olivine ± orthopyroxene ± chromite ± amphibole ± chlorite ± phlogopite (Fig. 3b). The olivine mode varies from ~88 to 98% whereas the other phases, except for orthopyroxene, are rarely present at modes >5%. Olivine is either equigranular or tabular, with the latter defining a pronounced lineation. Grain size varies from 0·1 mm to 2 cm, although large grains are rare and average grain size is ~0·4 mm. Some rare olivine grains reach 30 cm in long axis, and pseudomorphed grains (now represented as recrystallized olivine aggregates with parallel orientation) up to 80 cm long have been observed by the authors, indicating original large grain sizes in the mantle protolith. Orthopyroxene is present in several samples as large (>2 mm) strained porphyroclasts that make up <10% of the mode. These porphyroclasts are commonly brown and fibrous-looking, and attenuated parallel to the foliation.

Pale purple chlorite occurs as small discrete flakes (0·4–0·5 mm) or as ribbons of larger interlocking grains (0·5–1·0 mm in length) that are associated with trains of fine-grained (<0·5 mm) disseminated chromite. Large (~1 mm) grains of chromite are present in the matrix of some samples. Amphibole and phlogopite typically occur as single pale green flakes (lengths of <0·6 mm and <0·2 mm, respectively) in close association with chlorite.

ANALYTICAL METHODS

All analyses were carried out in the Geochemical Analysis Unit (GAU) at the ARC National Key Centre GEMOC in the Department of Earth and Planetary Sciences,

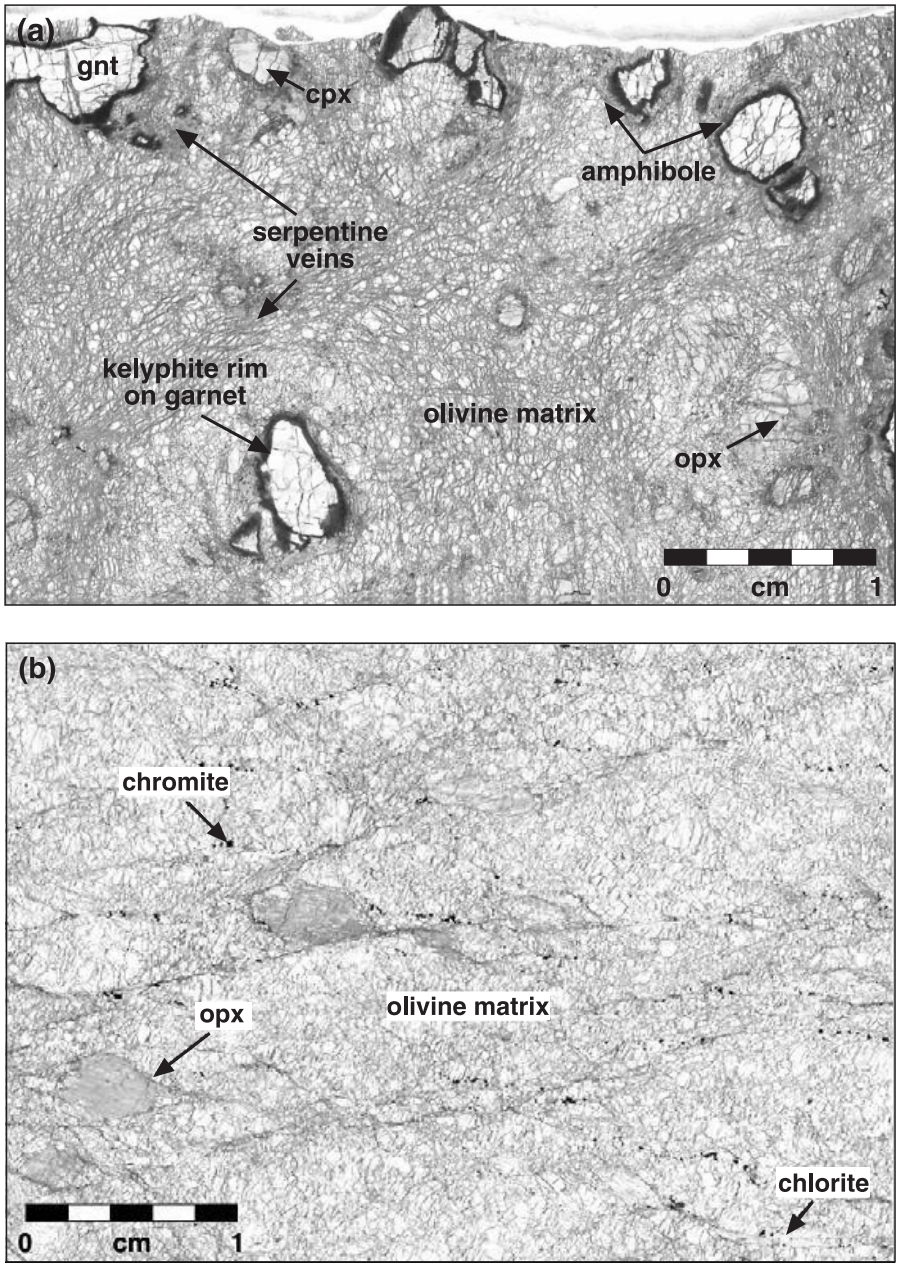

Fig. 3. Photomicrographs of peridotites from Almklovdalen. (a) Porphyroclastic texture in garnet lherzolite N97-14. Kelyphite rims and amphibole mantles are well developed on garnets. Serpentine veins are abundant and occasionally are observed cross-cutting porphyroclasts (see garnet grain in top left-hand corner). (b) Porphyroclastic texture in dunite N97-8. Large orthopyroxene porphyroclasts are set in a fine-grained olivine matrix.

Macquarie University. The major elements of whole-rock samples were analysed by X-ray fluorescence (XRF) using methods described by O'Reilly & Griffin (1988). International rock standards provided calibration for major elements and an appropriate range of international or internal standards was included as unknowns in each run. All samples were run in duplicate. FeO was determined by HF digestion and titration with ceric sulphate. H_2O^+ and CO_2 were determined using a LECO induction furnace whereas H_2O^- was determined separately by drying at 110°C for 2 h.

Trace elements in whole-rock samples were analysed in solution using inductively coupled plasma mass spectrometry (ICPMS). Rare earth elements (REE), large ion lithophile elements (LILE; Cs, Rb, Ba, Th, U, Sr), high field strength elements (HFSE; Nb, Ta, Zr, Hf), as well as

minor and transition elements (Ti, V, Cr, Ni, Cu, Zn, Ga, Mo) were analysed. The ICPMS instruments used were a Perkin Elmer Sciex Elan 6000 and a Hewlett Packard 4500 with a shield torch. For each batch, USGS and JGS rock standards have been included to check the accuracy of the analyses. Drift was corrected using ^{6}Li, Ru, In and Bi as doping elements.

Electron microprobe (EMP) analyses reported here were performed on a CAMEBAX SX50. A range of natural standards was used, together with standard matrix correction procedures. Count times used were 10 s for peaks with 5 s for backgrounds on either side of the peak.

Data on REE and selected other trace elements in mineral phases were acquired using the Laser Ablation Microprobe-ICPMS facility at GEMOC. This technique allows rapid and precise (<5%) *in situ* determination of trace-element abundances to sub-ppm levels (Norman *et al.*, 1996). The instrument consists of two parts; a laser ablation microprobe in which the sample is ablated, and an ICPMS where the ablated material is ionized and analysed. Two different lasers were used over the course of this study; an in-house system, based on a Continuum Surelite I-20 Q-switched laser, and designed by S. E. Jackson and H. Longerich, and a Merchantek LUV266. Both are frequency quadrupled Nd-YAG lasers with a beam wavelength of 266 nm and typical operating frequencies of 4–10 Hz. In both cases the beam is directed through a focusing lens onto the polished sample with a typical spot size of 50 μm. The ablated material is then carried from the sample chamber to the ICPMS by a stream of high-purity argon or helium. Analyses are generally made over 3–4 min with over 100 replicates. Each replicate is a sweep of the mass range with dwell times of 50–100 ms. Typically the first 40–60 s of the analysis are used to measure the background of the nebulizer gas before ablation is begun. Analyses are normalized to Ca or Mg contents previously determined by EMP. The external standards used were the NIST 610 and 612 glasses. Data reduction was carried out on-line using GLITTER, an interactive program developed by GEMOC (see http://www.es.mq.edu.au/GEMOC) which allows selection and integration of the most stable parts of each time-resolved signal.

WHOLE-ROCK COMPOSITION

Major elements

Mafic melt extraction from a primitive mantle source resulting in a residue is the common explanation for the trends seen in whole-rock major-element data for mantle peridotites. The residue is variously depleted in basaltic components such as Al_2O_3, CaO, TiO_2 and Na_2O. However, refertilization of an originally depleted source by melts rich in basaltic components (including Al, Ca, Fe) produces essentially the same trends.

The differences between the major-element abundances for the Almklovdalen peridotites and an estimate for primitive mantle (McDonough & Sun, 1995) are illustrated in Fig. 4 (see Table 1 for whole-rock major-element data). Mg-number values for the garnet peridotites range from 90·6 to 91·7, indicating that the garnet-bearing rocks are moderately to weakly refractory; that is, depleted in basaltic components, relative to primitive mantle. This is also reflected in the Al_2O_3 and CaO contents of the garnet peridotites. Na_2O abundances are fairly high in the garnet peridotites, close to or even higher than primitive mantle values, and reflect the presence of amphibole in these rocks. Cr-number ranges from 5 to 20 and shows an overall positive correlation with Mg-number.

In contrast, the dunites from Almklovdalen are strongly depleted, with Mg-number in the range 92–93·6 (Fig. 4). These rocks are extremely poor in Al and other magmaphile elements, consistent with their high modal olivine content and lack of Ca–Al-bearing phases such as garnet and clinopyroxene. Na_2O contents in the dunites range from zero to values comparable with those found in the garnet peridotites, and, as with the latter, this is attributed to the presence of amphibole in these rocks. There is a large range in Cr-number for the dunites that is controlled by variation in Al_2O_3, with the most depleted samples having the highest Cr-number.

High Mg-number coupled with strong depletion in Al_2O_3 and CaO like that seen in the Almkovdalen dunites is indicative of high degrees of partial melting. Similar levels of depletion have been observed in dunite xenoliths from Russia (Boyd & Finnerty, 1980), Tanzania (Rudnick *et al.*, 1993) and Greenland (Scott Smith, 1987; Bernstein *et al.*, 1998). Data for the 'mine run' dunites confirm that the bulk of the Almklovdalen body is very depleted (see Table 1). This is in contrast to olivine-rich rocks from other massifs and settings, which often have much lower bulk-rock Mg-number (i.e. <91); for example, those in massifs at Lanzo (Bodinier, 1988), Balmuccia (Shervais & Musaka, 1991) and Horoman (Takahashi 1986), and those in ophiolites, such as Oman (Godard *et al.*, 2000). Although it is generally agreed that most dunite is formed by melt extraction, it can also be formed by melt reaction processes or by crystallization from an ultramafic melt. The latter probably can be ruled out as there is no evidence for komatiitic or picritic lavas in the WGR, and the melt-reaction process tends to operate at small scales and is unlikely to have produced the huge volume of dunite seen at Almklovdalen.

The strong relationship between whole-rock Mg-number and Al_2O_3, CaO, Na_2O and Cr-number in the garnet peridotites suggests that they are linked by a common depletion or refertilization process. The argument for these trends reflecting refertilization rather than depletion is strengthened by the pseudo-mixing lines

Table 1: Whole-rock major-element (XRF) and trace-element (ICPMS) abundances for Almklovdalen peridotites

Sample no.:	N97-5	N97-6	N97-7	N97-8	N97-9	N97-11	N97-13	N97-14	N97-15	N97-16	N97-17	N97-18	N97-22	N97-23	N97-24	LNWG	ST89	ST95
Rock type:	gnt perid	dunite	dunite	dunite	dunite	dunite	dunite	gnt perid	gnt perid	gnt perid	dunite	gnt perid	dunite	dunite	dunite	gnt perid	dunite	dunite
wt %																		
SiO_2	42·9	41·6	41·8	43·6	43·6	41·1	44·2	42·3	41·2	42·2	40·8	44·3	46·6	42·4	42·0	44·6	41·8	42·0
TiO_2	0·05	0·00	0·01	0·00	0·00	0·00	0·01	0·04	0·02	0·04	0·01	0·01	0·01	0·01	0·01	0·07	0·00	0·00
Al_2O_3	1·93	0·10	0·06	0·15	0·54	0·00	0·23	2·92	1·78	2·38	0·12	2·32	0·00	0·00	0·00	3·28	0·38	0·09
Fe_2O_3	0·33	0·45	0·84	1·14	0·62	3·25	1·61	2·54	2·85	2·56	1·62	1·37	0·73	1·66	0·41	8·32	0·45	0·05
FeO	7·43	6·30	5·61	5·04	5·44	3·65	4·68	4·98	4·32	4·63	5·22	5·86	5·54	4·67	6·14	—	6·03	6·59
MnO	0·13	0·11	0·10	0·09	0·11	0·09	0·11	0·14	0·11	0·13	0·12	0·13	0·12	0·10	0·11	0·13	0·10	0·10
MgO	44·7	49·7	49·8	47·6	47·2	51·5	47·6	39·0	42·5	41·0	48·6	39·7	45·1	50·7	50·0	41·9	49·2	51·0
CaO	1·46	0·02	0·10	0·04	0·07	0·01	0·11	2·49	1·56	1·48	0·06	2·10	0·47	0·04	0·05	2·09	0·08	0·03
Na_2O	0·46	0·31	0·11	0·11	0·22	0·07	0·17	0·33	0·25	0·26	0·12	0·33	0·16	0·11	0·32	0·25	0·08	0·10
K_2O	0·02	0·02	0·03	0·02	0·01	0·01	0·01	0·01	0·02	0·01	0·01	0·01	0·01	0·01	0·00	0·00	0·01	0·00
Cr_2O_3	0·40	0·20	0·28	0·31	0·42	0·14	0·28	0·36	0·45	0·36	0·45	0·42	0·50	0·35	0·27	0·49	—	—
NiO	0·31	0·36	0·35	0·32	0·33	0·37	0·33	0·28	0·30	0·30	0·35	0·28	0·27	0·36	0·36	0·29	—	—
P_2O_5	0·01	0·00	0·01	0·01	0·01	0·01	0·01	0·02	0·03	0·02	0·01	0·02	0·02	0·01	0·01	0·03	0·00	0·00
H_2O^+	0·52	1·15	0·86	0·94	1·22	0·55	0·92	3·89	4·75	4·26	2·20	2·44	0·64	0·59	0·82	0·49	1·33	0·57
H_2O^-	0·06	0·07	0·09	0·07	0·10	0·06	0·05	0·20	0·14	0·28	0·25	0·30	0·12	0·08	0·08	0·03	0·06	0·02
CO_2	0·12	0·05	0·05	0·03	0·15	0·02	0·15	0·13	0·13	0·18	0·05	0·07	0·04	0·08	0·06	0·03	0·14	0·11
Sum	100·8	100·2	100·1	99·5	100·0	100·8	100·5	99·6	100·4	100·1	99·9	99·6	100·3	101·1	100·6	102·0	99·7	100·6
FeO (total)	7·73	6·70	6·37	6·07	6·00	6·57	6·13	7·27	6·88	6·93	6·68	7·09	6·20	6·16	6·51	7·49	7·15	7·38
Mg-no.	91·2	92·9	93·3	93·3	93·4	93·3	93·3	90·6	91·7	91·4	92·9	90·9	92·9	93·6	93·2	90·9	92·5	92·5
ppm																		
Sc	13	5·9	5·6	6·0	7·1	5·4	6·8	15	15	14	4·0	14	6·0	6·0	5·0	16	5·2	4·3
Ti	330	2·0	33	4·7	3·5	5·8	4·2	240	120	210	31	78	35	19	15	540	16	7·4
V	46	7·1	6·7	13	17	2·6	17	66	50	40	7·9	48	7·2	1·5	3·1	81	27	23
Cr	2280	660	550	940	1300	200	1140	2300	2350	2050	350	2180	570	66	240	1770	790	630
Co	110	130	97	120	96	130	120	100	110	90	110	98	92	120	110	94	120	110

Sample no.:	N97-5	N97-6	N97-7	N97-8	N97-9	N97-11	N97-13	N97-14	N97-15	N97-16	N97-17	N97-18	N97-22	N97-23	N97-24	LNWG	ST89	ST95
Rock type:	gnt perid	dunite	dunite	dunite	dunite	dunite	dunite	gnt perid	gnt perid	gnt perid	dunite	gnt perid	dunite	dunite	dunite	gnt perid	dunite	dunite
Ni	2360	2950	2660	2780	2340	2880	2610	1900	2240	1890	2450	1900	1810	2780	2380	2200	2810	2850
Ga	1·7	0·16	0·22	0·23	0·25	0·13	0·23	1·9	0·96	1·3	0·76	1·6	0·24	0·11	0·15	1·8	0·38	0·15
Rb	0·25	0·68	0·37	0·33	0·41	0·04	0·08	0·15	0·14	0·06	0·08	0·08	0·08	0·03	0·02	0·11	0·43	0·14
Sr	30·8	5·2	8·1	8·3	7·1	5·9	14	35	29	19	12	17	27	8·6	6·8	18	14	6·4
Y	2·1	0·02	0·07	0·01	0·02	0·01	0·02	2·7	1·4	1·4	0·13	1·7	0·05	0·03	0·03	3·4	0·10	0·01
Zr	1·8	0·09	0·12	0·04	0·07	0·04	0·11	2·5	1·2	1·3	0·2	0·43	0·15	0·07	0·06	3·2	0·30	0·07
Nb	0·41	0·09	0·23	0·07	0·08	0·09	0·07	0·24	0·26	0·2	0·13	0·55	0·18	0·29	0·22	1·2	0·16	0·08
Cs	0·1	0·05	0·04	0·03	0·03	0·01	0·01	0·03	0·01	0·02	0·04	0·01	0·01	0·01	0	0·02	0·06	0·02
Ba	46	12	6·8	12	4·2	1·1	2·6	15	13	4·7	2·2	12	0·81	1·1	0·28	22	18	4·1
La	1·3	0·05	0·20	0·07	0·10	0·03	0·09	0·19	0·13	0·12	1·1	1·9	0·36	0·21	0·09	1·5	0·42	0·15
Ce	2·7	0·09	0·43	0·07	0·21	0·06	0·20	1·1	0·54	0·49	0·19	2·4	1·1	0·31	0·15	3·3	0·65	0·09
Pr	0·16	0·01	0·04	0·01	0·02	0·005	0·02	0·24	0·13	0·11	0·16	0·22	0·10	0·022	0·02	0·39	0·07	0·01
Nd	0·34	0·03	0·15	0·02	0·06	0·02	0·07	1·5	0·88	0·72	0·61	0·74	0·27	0·06	0·05	1·3	0·22	0·04
Sm	0·10	0·005	0·03	0·003	0·01	0·003	0·01	0·47	0·28	0·23	0·07	0·08	0·02	0·01	0·01	0·19	0·04	0·008
Eu	0·06	0·004	0·01	0·004	0·003	0·001	0·004	0·14	0·08	0·06	0·01	0·03	0·01	0·002	0·002	0·08	0·01	0·003
Tb	0·04	b.d.	0·003	b.d.	0·001	b.d.	0·001	0·07	0·03	0·03	0·01	0·02	0·003	0·001	0·001	0·07	0·004	0·001
Gd	0·2	0·004	0·02	0·003	0·01	0·002	0·01	0·45	0·21	0·18	0·06	0·10	0·02	0·01	0·01	0·34	0·03	0·004
Dy	0·3	0·001	0·01	0·001	0·003	0·001	0·004	0·43	0·19	0·19	0·02	0·19	0·01	0·003	0·004	0·48	0·02	0·004
Ho	0·07	b.d.	0·002	b.d.	b.d.	b.d.	0·001	0·10	0·05	0·05	0·004	0·06	0·001	0·001	0·001	0·12	0·004	0·001
Er	0·21	0·002	0·01	0·001	0·001	0·001	0·002	0·29	0·14	0·15	0·01	0·19	0·004	0·003	0·003	0·36	0·01	0·002
Yb	0·22	0·004	0·01	0·003	0·003	0·003	0·003	0·29	0·17	0·19	0·01	0·22	0·01	0·01	0·01	0·37	0·01	0·004
Lu	0·03	0·001	0·002	0·001	0·001	0·001	0·001	0·05	0·03	0·03	0·002	0·04	0·001	0·001	0·001	0·06	0·002	0·001
Hf	0·05	b.d.	0·01	b.d.	b.d.	b.d.	b.d.	0·05	0·02	0·03	0·01	0·02	b.d.	b.d.	b.d.	0·10	0·008	0·002
Ta	0·01	b.d.	0·01	b.d.	b.d.	b.d.	b.d.	0·03	0·02	0·02	0·01	0·01	0·01	0·01	0·01	0·05	0·01	0·007
Pb	2·2	0·35	0·4	0·31	0·44	0·22	0·24	4·7	1·0	1·0	0·39	0·59	0·32	0·45	0·24	0·80	0·67	0·42
Th	0·1	0·01	0·07	0·01	0·01	0·01	0·01	0·01	0·01	0·01	0·02	0·06	0·01	0·12	0·01	0·09	0·11	0·009
U	0·02	0·02	0·02	0·02	0·01	0·01	b.d.	0·01	b.d.	b.d.	0·04	0·02	0·02	0·03	b.d.	0·01	0·05	0·009

b.d., below detection limit.

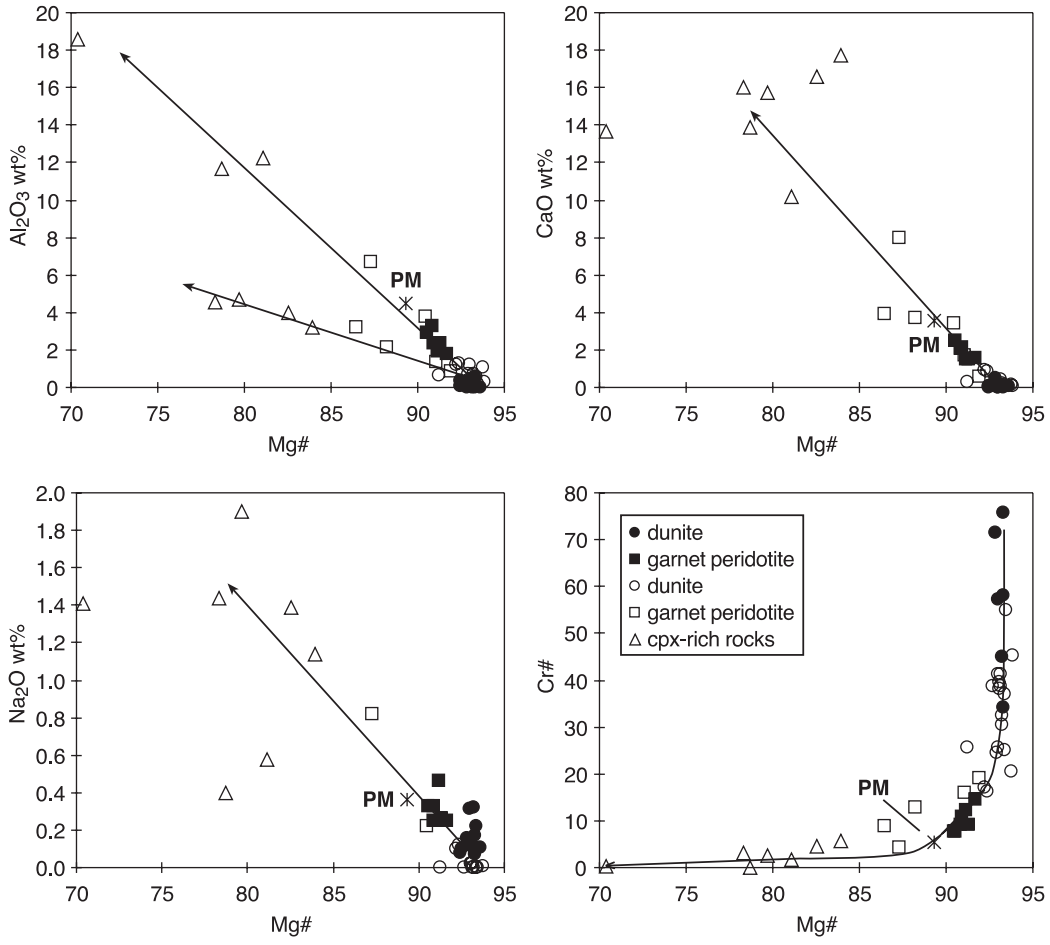

Fig. 4. Whole-rock major element oxides plotted against whole-rock Mg-number for peridotites from Almklovdalen. Filled symbols, this study; open symbols, published data. Published data taken from Eskola (1921), Mercy & O'Hara (1965*a*), Rost (personal communication, 1967), Finstadt & Heier (1972), Lappin (1974, 1975), Cordellier (1982), Griffin & Qvale (1985) and Osland (1997). Primitive mantle (PM) composition from McDonough & Sun (1995).

shown in each of the plots in Fig. 4. These lines suggest that the garnet-bearing peridotites are products of 'mixing' between the cpx-rich rocks and the depleted dunites; this is particularly apparent in the Mg-number vs Cr-number plot.

The garnet peridotites from Almklovdalen define a strong trend of increasing Al_2O_3 content with increasing CaO content (Fig. 5). The majority of these samples fall either in or adjacent to the field of Proterozoic lherzolite xenoliths (Griffin *et al.*, 1999*a*); the data taken from the literature show a great deal of scatter, with most samples showing significant enrichment in CaO. Conversely, several of the dunites fall in the field of Archaean peridotite xenoliths, and two samples have compositions close to the average for peridotite xenoliths in kimberlites of the Kaapvaal Craton. However, most of the dunites are highly depleted and lie below the Archaean field.

In conclusion, the whole-rock major-element data suggest that the olivine-rich rocks from the WGR, particularly those that are extremely poor in Al, cannot be simply retrograded garnet peridotites as suggested by Medaris (1984), but in fact are primary dunites and harzburgites.

Trace elements

A range of trace elements has been analysed in the garnet peridotites and dunites (Table 1). Ni is positively correlated with Mg-number in the suite. This is in contrast to the LILE, which show very poor correlation with Mg-number; the garnet peridotites show moderate enrichment in some of these elements compared with the dunites. The HFSE show variable behaviour. Zr and Hf show a weak negative correlation with Mg-number in the garnet peridotites whereas Nb and Ta do not: the highest concentrations of the latter occur in the amphibole-rich samples. The HFSE are all uniformly low in the dunites.

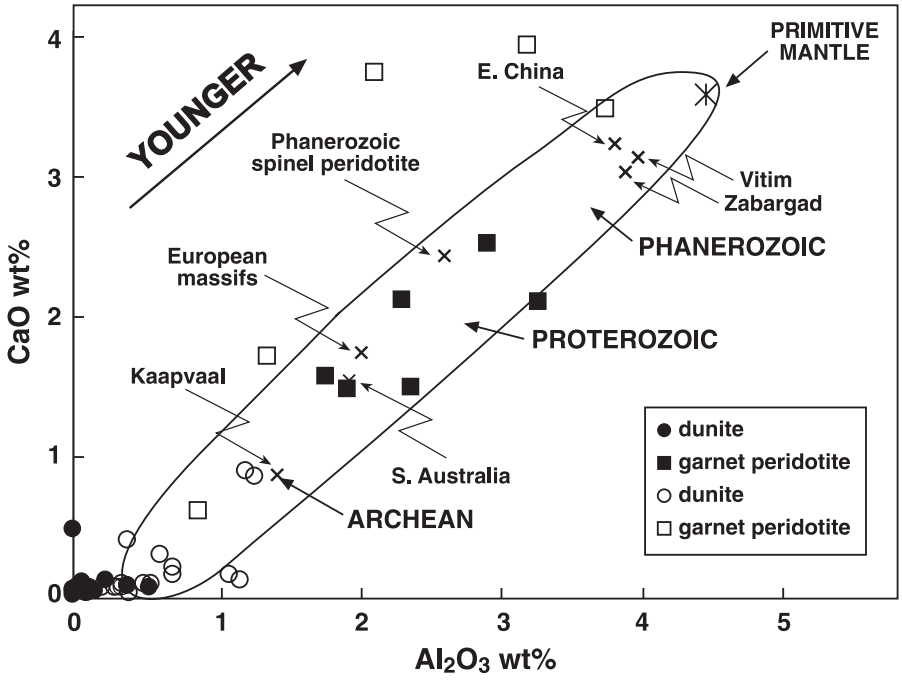

Fig. 5. Plot of Al_2O_3 vs CaO for Almklovdalen peridotites. Filled symbols, this study; open symbols, published data. Published data taken from Eskola (1921), Mercy & O'Hara (1965*a*), Rost (personal communication, 1967), Finstadt & Heier (1972), Lappin (1974, 1975), Cordellier (1982) and Osland (1997). Field taken from S. Y. O'Reilly & W. L. Griffin (personal communication); ×, xenolith averages (after O'Reilly *et al.*, 2001). Primitive mantle (PM) composition from McDonough & Sun (1995).

There is no correlation between light REE (LREE) abundances, represented by La, and Mg-number (Fig. 6). The garnet peridotites form two very distinct groups, one strongly enriched in La, the other depleted. The dunites have La contents (<0·5 ppm) comparable with those of the La-poor garnet peridotites.

The heavy REE (HREE) preferentially partition into garnet and it is thus expected that garnet-rich samples will be relatively enriched in these elements. This is evident in Fig. 6, which shows that the garnet peridotites have uniformly high Yb contents whereas the dunites contain negligible Yb. There is a very strong negative correlation between Yb and Mg-number (Fig. 6).

The REE patterns for the garnet peridotites can be divided into two distinct shapes: concave-down and concave-up (Fig. 7a). The concave-down patterns are defined by high middle REE (MREE) abundances [$(La/Nd)_N$ <1] relative to HREE and LREE whereas the concave-up patterns are LREE enriched [$(La/Nd)_N$ >1] relative to MREE, with LREE abundances varying from 0·02 × PM (primitive mantle) to 3 × PM in the most enriched samples (see Fig. 7a). Both of these patterns have previously been recognized in garnet peridotites from the Lien locality (Brueckner & Medaris, 1998; Medaris & Brueckner, 2003). The dunites are characterized by concave-up REE patterns (Fig. 8a) that have $(La/Yb)_N$ >1 and extremely low HREE abundances (~0·002–0·03 × PM). LREE enrichment in peridotite is commonly accompanied by enrichment in other incompatible elements such as the LILE, Th, and U. This is evident in the concave-up patterns of the garnet-bearing samples, which have overall higher abundances of Ba, Sr and Th than the peridotites with concave-down patterns (Fig. 7b). Enrichment in these elements and in the LREE has produced large negative anomalies in the HFSE in the garnet-bearing rocks. The dunites also show enrichment in the LREE and the LILE (Fig. 8b).

MINERAL CHEMISTRY

Olivine

Olivine grains in both the dunites and garnet lherzolites are unzoned and variation in Mg-number within an individual sample is less than ±0·2. Olivine Mg-number ranges from 90·5 to 93·5 (Fig. 9, Table 2) and compositional variation in olivine, and the other silicates, is primarily a reflection of the varying bulk-rock Mg-number, as documented by Medaris (1980). The relatively low Mg-number of the olivine (90·5–91·7) in the garnet peridotites contrasts strongly with the highly magnesian olivine (Mg-number 92·5–93·5) in the dunites from the same locality. This dichotomy in composition has already been identified in the whole-rock data

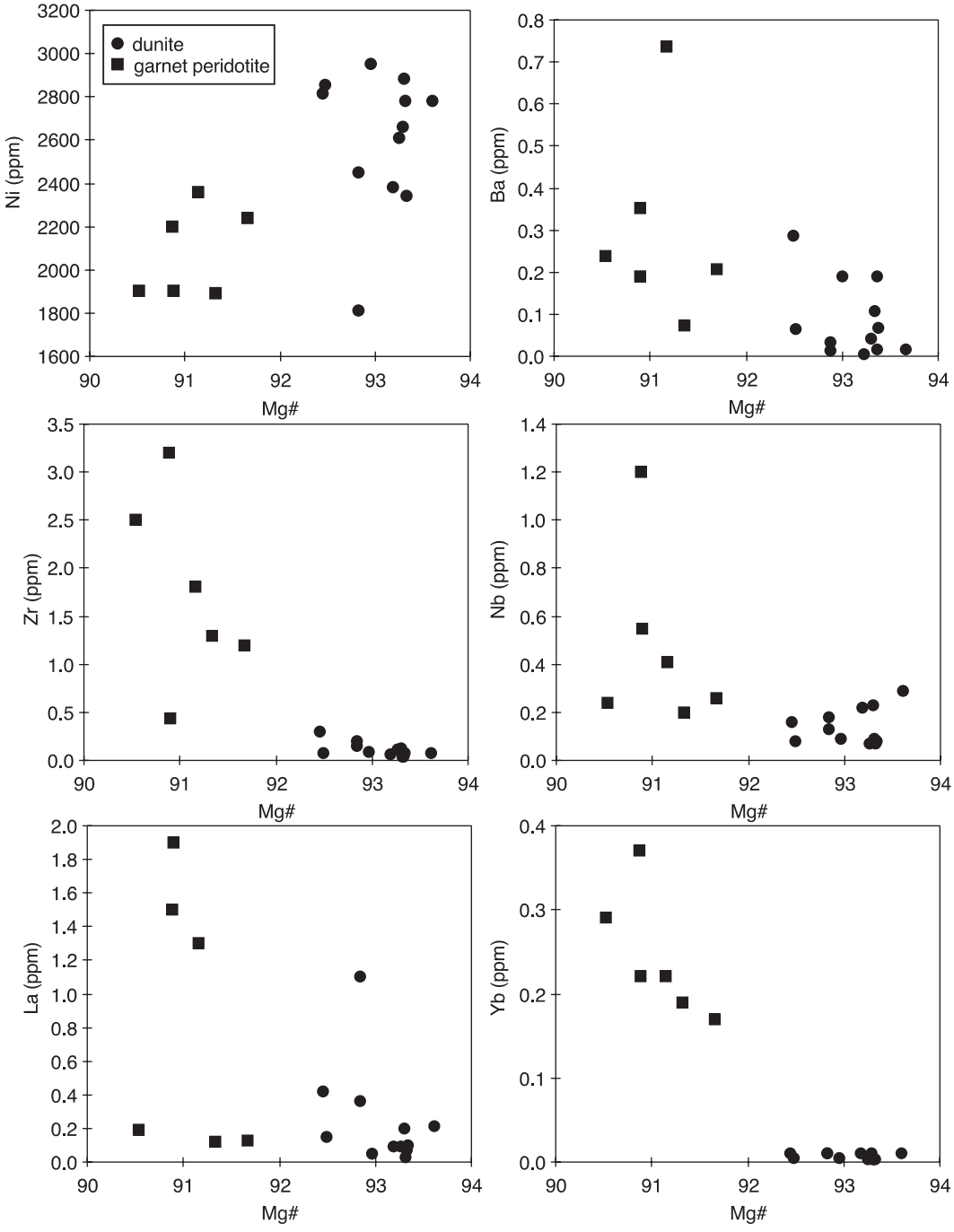

Fig. 6. Whole-rock trace-element abundances vs Mg-number for Almklovdalen peridotites.

(see Mg-number vs Cr-number plot in Fig. 4) and suggests a dichotomy in process.

Pyroxene

Orthopyroxene in the garnet peridotites has compositions that range from $En_{91·2}$ to $En_{92·1}$. A significant feature of the orthopyroxene is the consistently low, and uniform, content of Al_2O_3, which ranges from 0·67 to 0·73 wt %. Cr_2O_3 contents are low and vary from 0·12 to 0·19, and Cr-number is typically between 12 and 15 (Table 3). Orthopyroxenes from the dunites have homogeneous compositions with high Mg-number (92·5–93·5) and very low Al_2O_3 contents (0·06–0·5 wt %). These

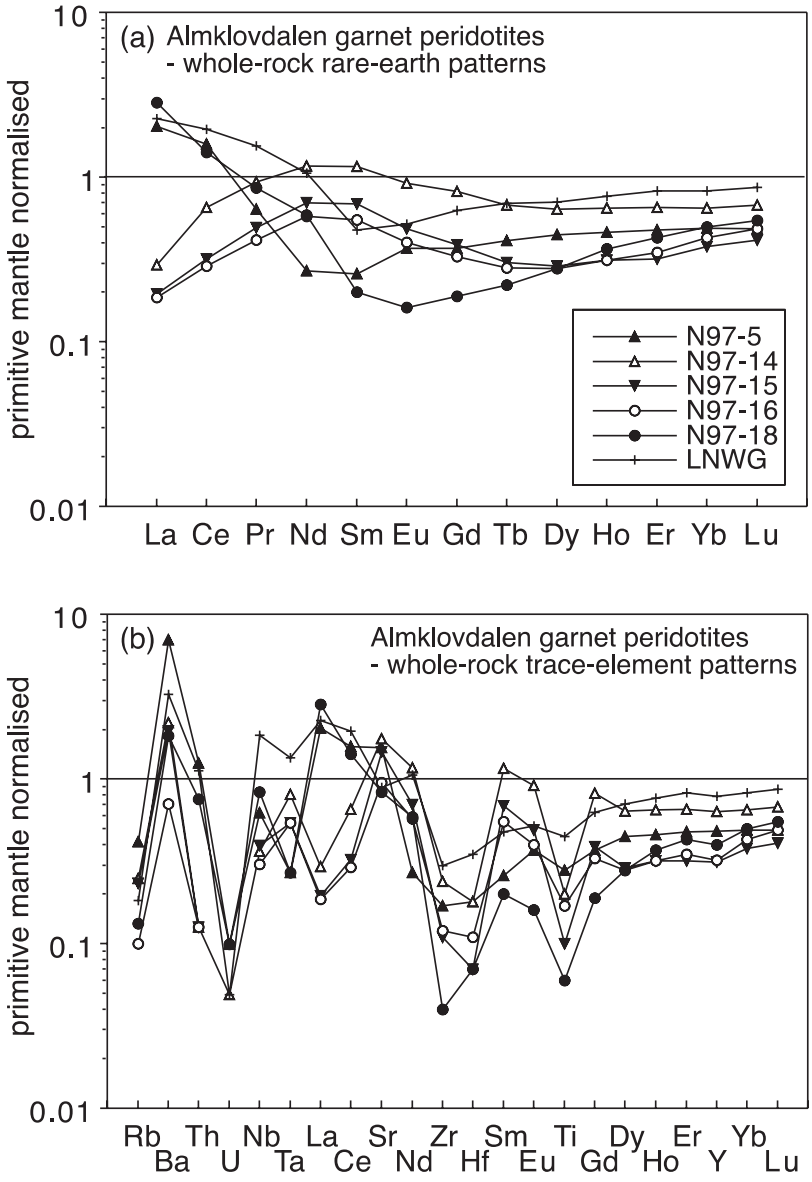

Fig. 7. Whole-rock primitive mantle normalized (a) REE and (b) trace-element patterns for Almklovdalen garnet peridotites.

orthopyroxenes have high Cr_2O_3 relative to Al_2O_3, compared with those in the garnet peridotites, and consequently have higher Cr-number.

Clinopyroxene from the garnet peridotites is diopside ($En_{47–50}Fs_{1·8–3·4}Wo_{48–51}$) characterized by high Al_2O_3, Na_2O and Cr_2O_3 but low MgO and CaO (Table 4). REE patterns for these clinopyroxenes show a range in shape from concave-up LREE and MREE, and low HREE abundances, to steep patterns with a negative slope that show a progression from LREE enrichment to depleted HREE (Fig. 10a). The similarity between these patterns and those for the whole-rock samples indicates that many of the trace elements in the latter are strongly controlled by the presence of clinopyroxene.

Garnet

The garnet in the lherzolites is Cr-pyrope (~67–69 mol % pyrope) and shows only small variations in grossular content (~11–13 mol %). Cr_2O_3 contents of the garnets range from 1·9 to 3·0 wt % (Table 4). On a CaO vs Cr_2O_3 plot (not shown) these compositions fall in the field for lherzolitic garnets. Cr-poor compositions, such as those seen in the WGR garnets, are characteristic of garnet from fertile to moderately depleted lherzolite

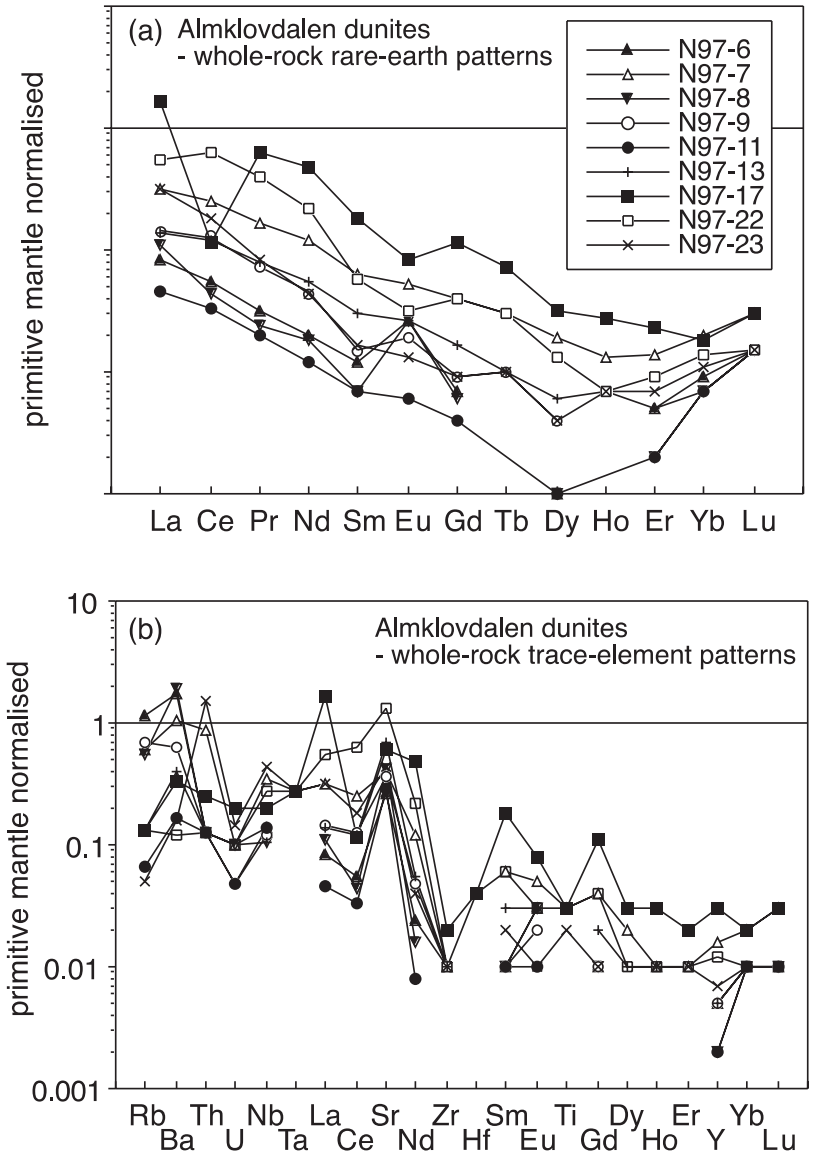

Fig. 8. Whole-rock primitive mantle normalized (a) REE and (b) trace-element patterns for Almklovdalen dunites.

(Griffin *et al.*, 1998). Garnets from the Almklovdalen peridotites have REE patterns characterized by flat HREE at high concentrations (5–7 × PM) and a sharp drop in REE abundances from Sm to Ce; a small enrichment in La is present in some samples (Fig. 11a).

REE studies of garnets from kimberlite-borne garnet lherzolite xenoliths have shown a range of REE patterns (Shimizu, 1975). Depleted garnets from harzburgite xenoliths (Nixon, 1987; Hoal *et al.*, 1994; Griffin *et al.*, 1999*a*, 1999*c*; van Achterbergh *et al.*, 2001; Carbno & Canil, 2002) and those that occur as inclusions in diamond (Shimizu & Richardson, 1987; Stachel *et al.*, 1998) typically have sinuous REE patterns that are depleted in HREE and LREE relative to the MREE. On the other hand, garnets from high-T sheared lherzolites and those from most fertile to mildly depleted garnet lherzolites have LREE-depleted patterns (Griffin *et al.*, 1989*a*, 1989*b*; Xu *et al.*, 2000) similar to the patterns seen in the Almklovdalen garnets.

The garnets from the Almklovdalen lherzolites have been classified according to the CARP (Cluster Analysis by Regressive Partitioning) scheme of Griffin *et al.* (2002). CARP is a statistical approach that has been used to define compositional populations within a large database of Cr-pyrope garnets from the subcontinental lithospheric mantle. The rules defining the populations (classes) are expressed in simple compositional variables

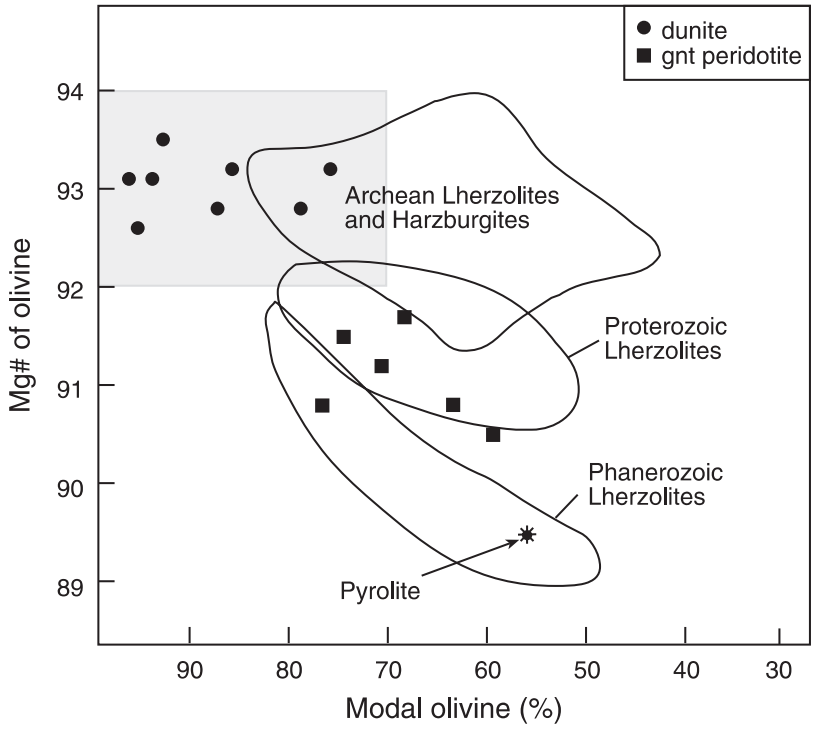

Fig. 9. Modal olivine vs olivine Mg-number for the Almklovdalen peridotites. Phanerozoic and Archean fields from Boyd (1989, 1997). Proterozoic field from Griffin *et al.* (1998). Grey field encloses data for olivine-rich peridotite xenoliths from Wiedemann Fjord (Greenland; Bernstein *et al.*, 1998), the Slave Craton (Boyd & Canil, 1997), the Tanzanian Craton (Lee & Rudnick, 1999) and Ubekendt Ejland (Greenland; Bernstein & Brooks, 1999).

Table 2: Major element abundances in olivines from the Almklovdalen peridotites

Sample no.:	N97-5	N97-6	N97-7	N97-8	N97-9	N97-11	N97-13	N97-14	N97-15	N97-16	N97-17	N97-18	LNWG	N97-22	N97-23	N97-24
Rock type:	gnt lherz	dunite	dunite	dunite	dunite	dunite	dunite	gnt lherz	gnt lherz	gnt lherz	dunite	gnt lherz	gnt lherz	dunite	dunite	dunite
SiO_2	40·6	40·2	40·3	40·7	41·1	41·1	41·9	41·0	40·9	41·53	41·0	41·5	41·2	41·3	41·9	41·9
TiO_2	0·01	0·01	0·01	0·01	0·00	0·00	0·00	0·02	0·02	0·01	0·01	0·01	0·01	0·00	0·01	0·01
Al_2O_3	0·00	0·00	0·01	0·00	0·01	0·01	0·00	0·01	0·00	0·00	0·00	0·00	0·00	0·00	0·01	0·00
Cr_2O_3	0·01	0·01	0·02	0·01	0·02	0·02	0·03	0·02	0·01	0·01	0·01	0·01	0·01	0·01	0·01	0·01
FeO	9·12	7·19	6·89	6·95	6·74	6·74	7·12	9·08	8·33	8·25	7·31	8·25	8·56	7·40	6·67	6·89
MnO	0·12	0·11	0·11	0·11	0·09	0·09	0·10	0·12	0·13	0·09	0·11	0·09	0·11	0·12	0·09	0·11
MgO	50·3	51·8	52·1	51·9	51·8	51·8	51·7	50·0	50·6	50·9	51·3	50·9	49·5	51·1	52·2	51·8
CaO	0·00	0·01	0·01	0·00	0·01	0·01	0·01	0·01	0·01	0·01	0·01	0·01	0·00	0·01	0·01	0·01
Na_2O	0·00	0·00	0·00	0·00	0·00	0·00	0·00	0·00	0·00	0·00	0·01	0·00	0·01	0·00	0·00	0·00
K_2O	0·00	0·00	0·00	0·01	0·01	0·01	0·01	0·01	0·00	0·01	0·00	0·01	0·00	0·01	0·00	0·00
NiO	0·43	0·39	0·39	0·44	0·41	0·41	0·01	0·40	0·39	0·41	0·41	0·41	0·40	0·42	0·41	0·40
Sum	100·6	99·8	99·9	100·1	100·3	100·2	101·3	100·8	100·4	101·2	100·2	101·5	99·8	100·4	101·3	101·1
Mg-no.	90·8	92·8	93·1	93·0	93·2	93·1	92·8	90·8	91·5	91·7	92·6	90·5	91·2	92·5	93·3	93·1

(major oxides, Ga, Sr, Y and Zr) and are therefore applicable to new samples and other databases (Griffin *et al.*, 2002). The classes are divided into four groups: Group 1 (depleted harzburgites and lherzolites, little metasomatism); Group 2 (depleted, metasomatized (± phlogopite) lherzolites]; Group 3 [fertile to moderately depleted (metasomatized) lherzolites]; Group 4 (melt-related metasomatism).

Table 3: Major element abundances in orthopyroxenes from the Almklovdalen peridotites

Sample no.:	N97-5	N97-6	N97-8	N97-13	N97-15	N97-16	N97-18	N97-14	LNWG	N97-21	N97-22	N97-23
Rock type:	gnt perid	dunite	dunite	dunite	gnt perid	gnt perid	gnt perid	gnt perid	gnt perid	dunite	dunite	dunite
SiO_2	57·5	57·6	58·0	59·13	57·7	58·9	58·5	58·3	58·3	58·7	58·6	59·1
TiO_2	0·03	0·00	0·01	0·00	0·02	0·03	0·03	0·01	0·03	0·01	0·02	0·01
Al_2O_3	0·67	0·07	0·12	0·27	0·73	0·67	0·69	0·60	0·59	0·50	0·08	0·06
Cr_2O_3	0·17	0·10	0·09	0·18	0·18	0·14	0·19	0·12	0·13	0·14	0·05	0·04
FeO	6·00	5·15	4·75	4·97	5·34	5·47	5·83	6·15	5·72	4·84	5·16	4·59
MnO	0·13	0·18	0·13	0·12	0·11	0·10	0·10	0·12	0·12	0·14	0·14	0·12
MgO	35·7	36·5	36·8	36·4	35·8	35·9	35·6	35·5	34·8	36·7	36·2	36·9
CaO	0·12	0·08	0·09	0·11	0·11	0·11	0·12	0·11	0·10	0·14	0·09	0·08
Na_2O	0·00	0·00	0·01	0·00	0·00	0·00	0·00	0·00	0·01	0·02	0·00	0·00
K_2O	0·00	0·00	0·00	0·01	0·00	0·01	0·01	0·01	0·00	0·01	0·00	0·00
NiO	0·07	0·04	0·09	0·01	0·07	0·05	0·06	0·07	0·09	0·07	0·07	0·06
Total	100·4	99·8	100·1	101·3	100·1	101·3	101·1	101·0	99·9	101·2	100·4	100·9
Mg-no.	91·4	92·7	93·2	92·9	92·3	92·1	91·6	91·1	91·6	93·1	92·6	93·5

The Almklovdalen garnets fall into CARP classes L9 and L10A of Griffin *et al.* (2002) and thus belong to their Group 3. Class L9 includes low-Cr garnets from very fertile lherzolites (low-Fo olivine), which may have been subjected to Fe-metasomatism. L9 garnets are characterized by high HREE and low LREE, consistent with relatively low degrees of depletion. Class L10A is typical of garnets from a range of fertile to moderately depleted lherzolites, many of which show evidence for phlogopite-related, or in some cases Ca + Al-dominated, metasomatism. These rocks contain abundant cpx and garnet, but have more magnesian olivine (mean = Fo_{92}). The REE patterns of L10A garnets are similar to those of L9 garnets. The lack of K enrichment in the Almklovdalen peridotites that fall in Class L10A suggests that these rocks have not been affected by phlogopite-related metasomatism but their high Ca and Al abundances (see Fig. 5) suggest metasomatism by a fluid rich in Ca and Al.

Chromite

Chromites in the garnet peridotites from Almklovdalen have Mg-number in the range 36–46 and Cr-number of 57–67 (Table 5). Chromites from the dunites are characterized by low Mg-number (22–35) and high-Cr-number (89–94) (Fig. 12).

Amphibole

Amphibole is widespread in both the garnet-bearing peridotites and the dunites. In the garnet peridotites amphibole occurs predominantly as partial rims around garnet whereas in the dunites it appears in association with chlorite. The amphiboles are calcic (CaO contents 11·2–13·0 wt %) although there is significant variation in composition between the different rock types (Table 4). Amphibole in the garnet peridotites is pargasite but compositions tend towards magnesio-hornblende. In the dunites, amphibole is tremolite, high in Si and very poor in alkalis.

Amphibole Mg-number varies with rock type as do the other silicates. The dunites contain amphibole with uniformly high Mg-number (94·1–96·4) compared with those in the garnet-bearing rocks which have Mg-number as low as 90 (Table 6). Trace elements in amphiboles from the garnet peridotites show a very strong similarity to REE and trace-element patterns for the whole-rock samples, suggesting that amphibole, in conjunction with clinopyroxene as discussed above, exerts a significant control on whole-rock trace-element abundances.

MODELLING OF DEPLETION PROCESSES

The extraction of mafic and ultramafic melts from fertile peridotite results in a depleted residue, the composition of which is determined by the initial peridotite composition and the melt composition at the conditions of segregation. Assuming that the rocks are the product of simple melt extraction, the degree of melting in the WGR peridotites can be estimated by comparing their major element and modal compositions with residue trends derived from melting experiments, over a pressure range of 3–7 GPa, on fertile peridotite KR4003 (Walter,

Table 4: Major- and trace-element abundances in clinopyroxene, garnet and amphibole from the Almklovdalen garnet peridotites

Sample no.:	N97-14	N97-15	N97-16	N97-18	LNWG	N97-5	N97-14	N97-15	N97-16	N97-18	LNWG	N97-5	N97-14	N97-15	N97-16	N97-18	LNWG
Mineral:	cpx	cpx	cpx	cpx	cpx	garnet	garnet	garnet	garnet	garnet	garnet	amph	amph	amph	amph	amph	amph
SiO_2	54·6	54·5	54·9	55·30	55·2	41·4	41·6	41·3	41·9	42·0	41·9	46·6	45·7	45·4	46·6	44·9	45·6
TiO_2	0·09	0·09	0·10	0·04	0·17	0·06	0·04	0·05	0·06	0·02	0·06	0·31	0·28	0·18	0·27	0·09	0·28
Al_2O_3	2·52	2·62	2·40	2·63	3·34	21·9	21·8	21·1	21·5	21·8	22·1	11·5	12·2	12·7	11·8	13·9	12·8
Cr_2O_3	1·26	1·77	1·59	1·47	1·65	2·30	1·92	3·02	2·42	2·14	2·12	1·54	1·18	1·30	1·60	1·67	1·52
FeO	1·96	1·56	1·66	1·62	1·60	9·69	9·68	8·91	9·71	10·3	9·65	2·81	3·67	3·44	3·00	3·13	3·07
MnO	0·03	0·02	0·03	0·03	0·04	0·43	0·45	0·44	0·46	0·47	0·45	0·03	0·03	0·06	0·03	0·03	0·07
MgO	15·5	15·4	15·8	15·60	14·7	19·9	19·4	19·6	19·3	19·1	18·8	19·0	18·4	18·3	18·8	18·0	18·8
CaO	22·0	21·6	21·9	21·93	21·1	4·70	4·81	5·21	4·93	4·80	4·73	12·6	12·7	12·3	12·5	12·5	11·9
Na_2O	1·69	1·85	1·60	1·76	2·33	0·02	0·02	0·01	0·02	0·01	0·02	2·07	2·10	1·92	2·19	2·67	2·86
K_2O	0·00	0·01	0·01	0·01	0·00	0·00	0·00	0·01	0·00	0·00	0·01	0·10	0·12	0·41	0·20	0·03	0·04
NiO	0·02	0·05	0·02	0·03	0·07	0·02	0·01	0·01	0·02	0·03	0·01	0·09	0·12	0·08	0·13	0·08	0·09
Total	99·7	99·5	100·0	100·4	100·2	100·4	99·8	99·5	100·3	100·7	99·8	96·6	96·6	96·0	97·1	97·1	97·0
Mg-no.	93·4	94·6	94·4	94·5	94·2	78·5	78·1	79·6	78·0	76·8	77·6	92·0	89·9	90·4	91·8	91·1	91·6
Ni	300	270	280	280	230	11	8·8	13	13	10	10	770	820	680	790	840	730
Ga	7·8	4·9	6·4	5·0	9·1	7·7	6·6	4·6	5·4	4·6	7·1	14	14	7·5	13	12	35
Rb	—	—	—	—	0·03	—	—	—	—	—	—	—	—	—	—	—	1·43
Ba	—	—	—	—	0·68	—	—	—	—	—	—	—	—	—	—	—	170
Th	0·07	0·05	0·03	0·22	0·31	0·02	<0·02	0·01	<0·02	0·02	<0·005	0·18	0·03	0·02	0·02	0·06	0·10
U	0·03	0·01	0·009	0·05	0·05	0·02	0·01	0·002	0·01	0·03	0·007	0·04	0·02	0·01	0·01	0·07	0·04
Nb	0·15	0·34	0·26	0·15	0·61	0·03	0·03	0·04	0·03	0·05	0·09	2·4	2·7	4·7	2·1	9·1	2·4
Ta	0·06	0·07	0·02	0·03	0·008	<0·02	<0·02	0·01	<0·02	0·01	<0·005	0·06	0·23	0·37	0·18	0·17	0·08
La	2·2	2·1	2·4	20	15	0·03	0·02	<0·02	0·02	0·07	0·02	13	2·2	1·5	2·1	19	9·5
Ce	11	9·2	8·7	26	36	0·13	0·05	0·04	0·03	0·12	0·13	30	12	7·6	9·6	30	30
Sr	320	310	310	140	160	0·04	0·16	0·13	0·11	0·07	0·21	200	310	310	270	160	150
Nd	17	16	16	8·3	13	0·18	0·67	0·86	0·61	0·47	0·43	5·2	19	16	20	11	13
Zr	16	9	10	1·9	21	11	10	6·1	6·0	1·5	9·2	14	12	13	13	3·3	17
Hf	0·52	0·30	0·41	0·11	1·1	0·17	0·11	0·08	0·09	0·06	0·13	0·68	0·47	0·38	0·54	0·13	0·77
Sm	4·9	3·4	3·4	0·69	1·5	0·33	0·98	1·2	0·92	0·22	0·35	1·5	5·1	4·4	5·0	1·0	1·7
Eu	0·98	0·70	0·70	0·16	0·47	0·25	0·51	0·49	0·39	0·12	0·22	0·59	1·5	1·1	1·1	0·27	0·56
Ti	820	500	890	230	1510	470	290	200	350	120	480	1680	1440	1170	1550	600	1990
Gd	1·8	1·2	1·2	0·38	1·4	1·3	1·9	1·4	1·1	0·47	1·3	2·0	3·1	2·2	2·0	0·73	1·77
Dy	0·57	0·31	0·33	0·28	0·65	2·9	2·7	1·8	1·7	1·7	2·9	2·0	1·9	1·2	0·87	0·89	1·4
Ho	0·07	0·04	0·04	0·04	0·09	0·74	0·63	0·49	0·40	0·50	0·74	0·40	0·36	0·23	0·15	0·19	0·24
Er	0·12	0·08	0·09	0·08	0·15	2·1	1·8	1·4	1·3	1·8	2·4	1·1	0·91	0·56	0·34	0·49	0·60
Y	1·6	0·98	1·1	0·95	1·9	18	17	12	10	13	19	10	9·2	5·5	3·7	4·8	6·0
Yb	0·06	0·06	0·05	0·06	0·06	2·6	2·1	1·9	1·8	2·4	2·8	0·96	0·81	0·53	0·32	0·40	0·40
Lu	<0·014	0·01	<0·015	0·02	0·007	0·40	0·32	0·32	0·31	0·38	0·43	0·13	0·11	0·07	0·05	0·06	0·05

1998). KR4003 is close in composition to peridotite KLB-1 (Takahashi, 1986), and to both pyrolite model compositions and peridotites from Zabargad that may represent fertile oceanic upper mantle (Bonatti *et al.*, 1986; McDonough & Sun, 1995). Figure 13 shows the residual trends for melting of pyrolitic mantle and a mixing trend between olivine and orthopyroxene (Walter, 1998). The fields for low-temperature and high-temperature garnet peridotites from the Kaapvaal and Siberia Cratons are shown for comparison.

Low-temperature cratonic peridotites lie along an olivine–orthopyroxene mixing trend, consistent with a

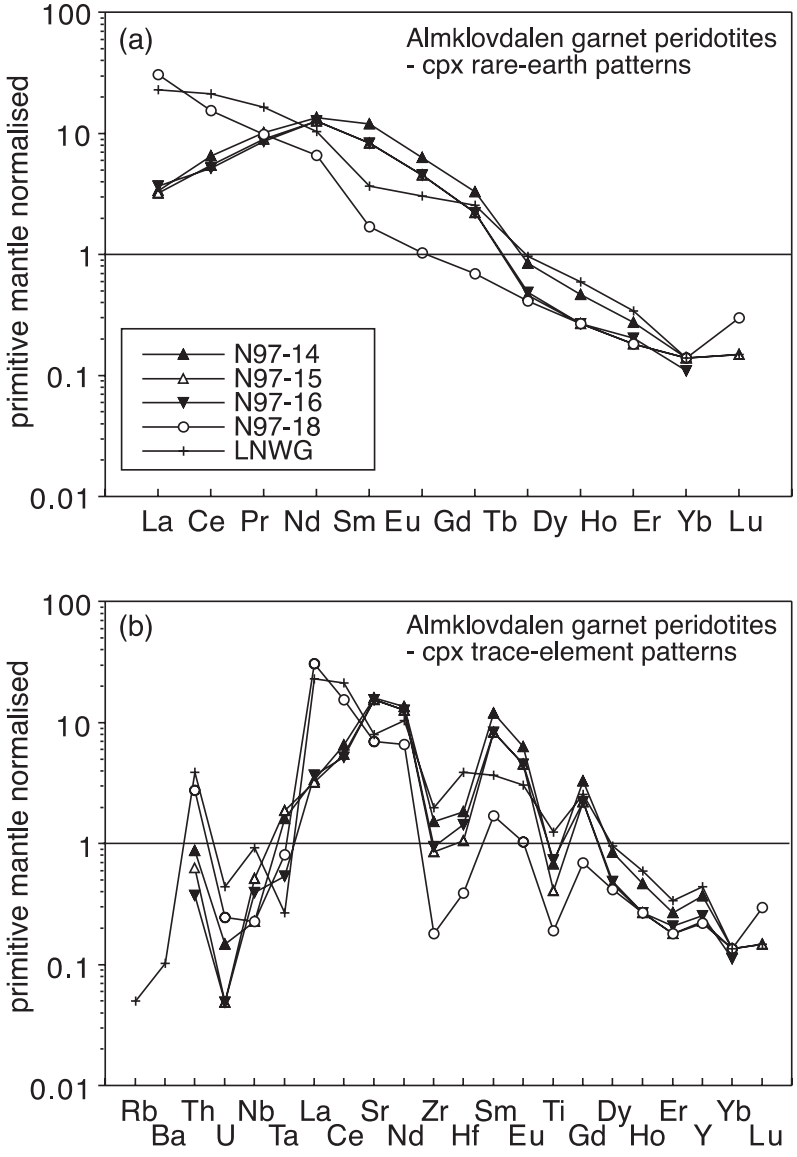

Fig. 10. Primitive mantle normalized (a) REE and (b) trace-element patterns of clinopyroxene in garnet peridotites from Almklovdalen.

melt-reaction process whereby olivine is consumed and orthopyroxene is crystallized, or with a mechanical sorting process. In contrast, data for the high-temperature sheared peridotites plot close to the residual melting trend for pyrolitic mantle. However, a large body of chemical and isotopic data shows that these sheared peridotites are not single-stage melting residues. Instead, their compositions reflect the refertilization of depleted lithospheric mantle by introduction of asthenosphere-derived melts, commonly shortly before kimberlite eruption (e.g. Harte, 1983; Griffin *et al.*, 1989*b*; Smith *et al.*, 1993; and references therein). The implied conditions of melt extraction for the high-T peridotites therefore are not meaningful.

Most of the dunites plot at the intersection of the 'residue' and 'mixing' trends but several samples have higher SiO_2 contents and lie along the mixing trend within the field for low-temperature peridotites. This coincidence emphasizes the similarity between the dunites and the depleted cratonic mantle peridotites seen in some xenolith suites from Archaean cratons. The Norwegian garnet peridotite data, in contrast, do not follow the mixing trend shown by the dunites, but are distributed about the 'residue trend'; they more closely resemble the high-T sheared peridotites.

Figure 14 shows whole-rock Mg-number vs modal olivine and modal orthopyroxene, relative to pyrolite residue trends for melting from 2 to 7 GPa (Walter,

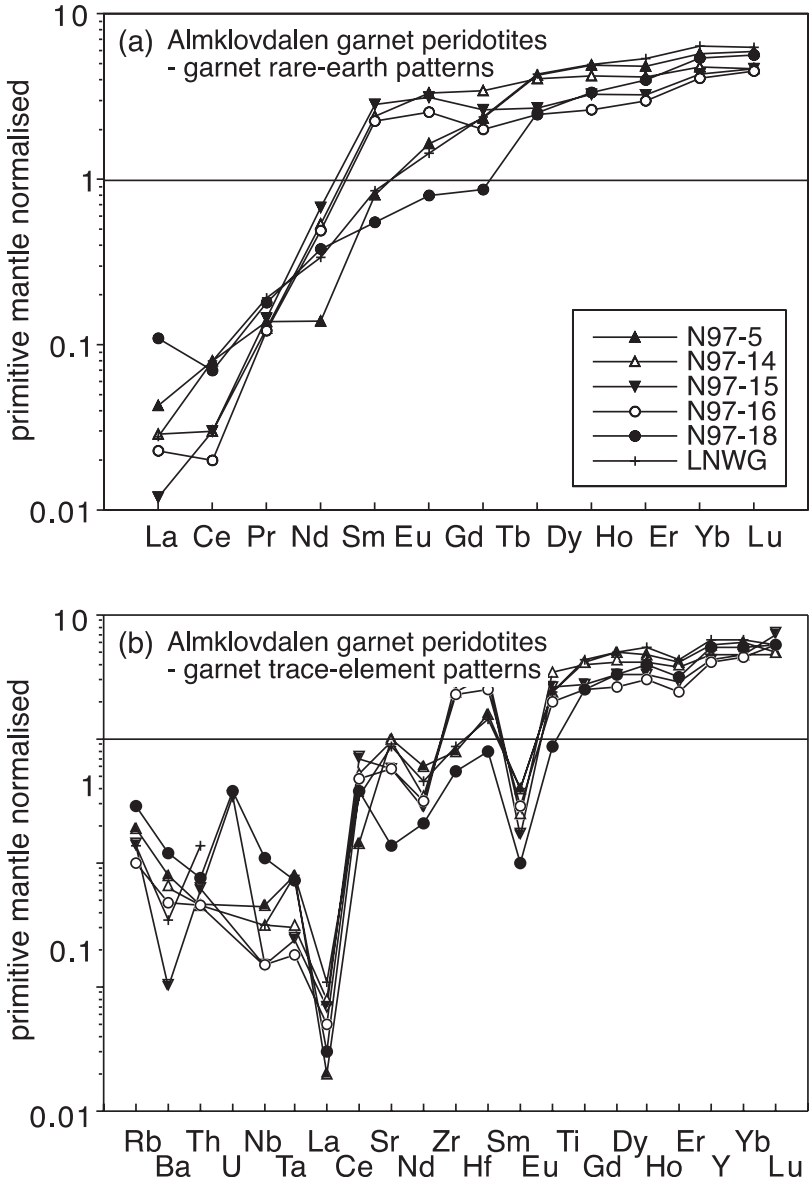

Fig. 11. Primitive mantle normalized (a) REE and (b) trace-element patterns of garnet in garnet peridotites from Almklovdalen.

1998). The extremely refractory compositions of the dunites suggest that they have been derived by very high degrees of partial melting (50–60%) at high pressure (3–7 GPa). They are thus more depleted than the mean low-temperature Archaean peridotite xenoliths from South Africa and Siberia. The garnet peridotite data, taken at face value, would imply more limited degrees of melting; Fig. 14b would indicate a relatively shallow melt-extraction regime (~2 GPa), whereas Fig. 14a would allow a wider range of pressures (2·5 to >5 GPa). Two of the samples lie close to the 'oceanic' trend in Fig. 14a, as do high-T peridotites from the Kaapvaal and Siberia Cratons (Walter, 1998).

DISCUSSION

There is a distinct difference in whole-rock and mineral compositions between the dunites and the garnet peridotites. The dunites are highly refractory (Mg-number >94) and appear to be the products of high degrees of melting (>60%). These high degrees of melting are similar to those seen in some other dunite suites from Archaean mantle. In Fig. 9, the WGR dunites fall in the field defined by olivine-rich rocks from Wiedemann Fjord (Bernstein *et al.*, 1998) and Ubekendt Ejland (Bernstein & Brooks, 1999) in Greenland, the Canadian Slave Craton (Boyd & Canil, 1997) and the Tanzanian Craton (Rudnick *et al.*, 1993; Lee & Rudnick, 1999). The

Table 5: Major element abundances in chromites from the Almklovdalen peridotites

Sample no.:	N97-5	N97-6	N97-7	N97-8	N97-9	N97-11	N97-13	N97-15	N97-16	N97-17	N97-21	N97-22	N97-23	N97-24
Rock type:	gnt perid	dunite	dunite	dunite	dunite	dunite	dunite	gnt perid	gnt perid	dunite	dunite	dunite	dunite	dunite
SiO_2	0·01	0·01	0·27	0·01	0·02	0·01	0·01	0·04	0·05	0·00	0·02	0·02	0·01	0·04
TiO_2	0·16	0·01	0·22	0·01	0·02	0·04	0·00	0·12	0·10	0·14	0·08	0·16	0·09	0·14
Al_2O_3	16·4	2·61	3·04	2·70	3·25	3·01	2·75	16·0	22·0	3·18	3·17	3·39	5·00	4·33
Cr_2O_3	49·2	58·4	56·9	59·9	59·5	57·9	62·1	47·2	43·4	57·7	59·4	58·2	59·4	56·8
FeO	24·0	31·3	29·7	28·5	26·8	29·2	27·9	25·4	21·3	30·1	29·2	29·3	25·5	30·1
MnO	0·00	0·00	0·00	0·00	0·00	0·41	0·00	0·00	0·00	0·00	0·00	0·00	0·00	0·00
MgO	8·28	5·06	6·00	5·22	6·32	6·21	5·04	8·17	10·4	6·00	5·39	6·27	7·65	6·11
CaO	0·00	0·00	0·01	0·00	0·01	0·01	0·01	0·02	0·00	0·01	0·02	0·01	0·00	0·01
Na_2O	0·01	0·04	0·03	0·02	0·01	0·00	0·02	0·00	0·03	0·02	0·01	0·00	0·01	0·02
K_2O	0·01	0·01	0·05	0·01	0·00	0·00	0·01	0·01	0·00	0·01	0·00	0·00	0·01	0·01
NiO	0·04	0·03	0·05	0·06	0·05	0·03	0·00	0·04	0·11	0·06	0·03	0·06	0·04	0·07
Sum	98·0	97·3	96·2	96·4	96·1	97·2	97·9	97·0	97·3	97·2	97·4	97·5	97·7	97·5
Mg-no.	38·1	22·5	26·4	24·6	29·6	27·5	24·4	36·4	46·4	26·3	24·7	27·6	35·0	26·6
Cr-no.	66·9	93·8	92·6	93·7	92·5	92·8	93·8	66·4	57·0	92·4	92·6	92·0	89·1	89·8

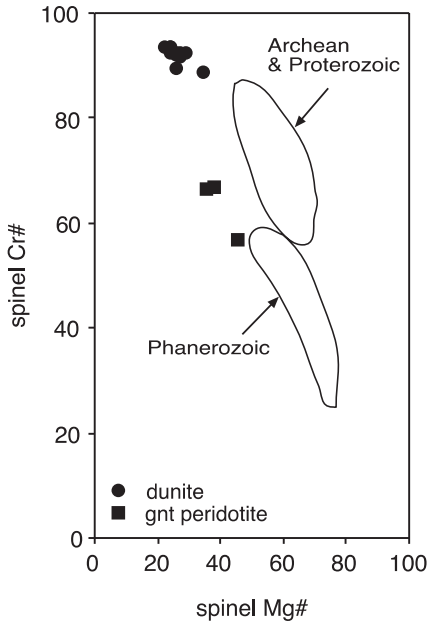

Fig. 12. Compositional variation diagrams for chromites from the Almklovdalen peridotites. Fields are from Yao (1999).

Table 6: Major element abundances in amphibole from the Almklovdalen dunites

Sample no.:	N97-7	N97-8	N97-9	N97-13	N97-17	N97-22 (1)	N97-22 (2)	N97-23
SiO_2	53·7	52·9	53·3	53·5	52·7	58·2	54·8	55·7
TiO_2	0·14	0·01	0·01	0·00	0·07	0·03	0·08	0·07
Al_2O_3	3·35	3·93	4·07	4·40	4·58	0·65	3·71	2·99
Cr_2O_3	0·79	1·00	0·86	1·24	1·04	0·21	0·54	0·58
FeO	2·21	2·51	2·48	2·48	2·44	1·59	2·23	2·03
MnO	0·06	0·05	0·05	0·04	0·04	0·04	0·04	0·06
MgO	23·0	22·8	22·7	22·2	22·4d	23·7	22·7	23·2
CaO	11·8	11·2	11·7	11·9	11·5	12·6	12·1	11·8
Na_2O	1·02	1·05	1·03	1·27	1·25	0·36	1·22	1·17
K_2O	0·46	0·59	0·50	0·42	0·71	0·05	0·35	0·35
NiO	0·06	0·06	0·11	0·01	0·12	0·09	0·13	0·13
Sum	96·6	96·2	96·9	97·5	96·9	97·5	98·0	98·1
Mg-no.	94·9	94·2	94·2	94·1	94·2	96·4	94·8	95·3

Archaean spinel dunites from Weidemann Fjord are extremely depleted and have been modelled as residues after ~40% melting of a primitive mantle source (Bernstein *et al.*, 1998).

In contrast, the garnet-bearing rocks from Almklovdalen are comparatively fertile. In particular, their whole-rock compositions show them to be only moderately depleted compared with primitive mantle, with high CaO and Al_2O_3 contents and Mg-number <92.

There is strong evidence for post-depletion modification of both the dunites and the garnet peridotites. The concave-up and concave-down REE patterns in the garnet-rich rocks do not resemble the LREE-depleted patterns typical of residual peridotite and suggest at least one episode of metasomatism by a melt or fluid

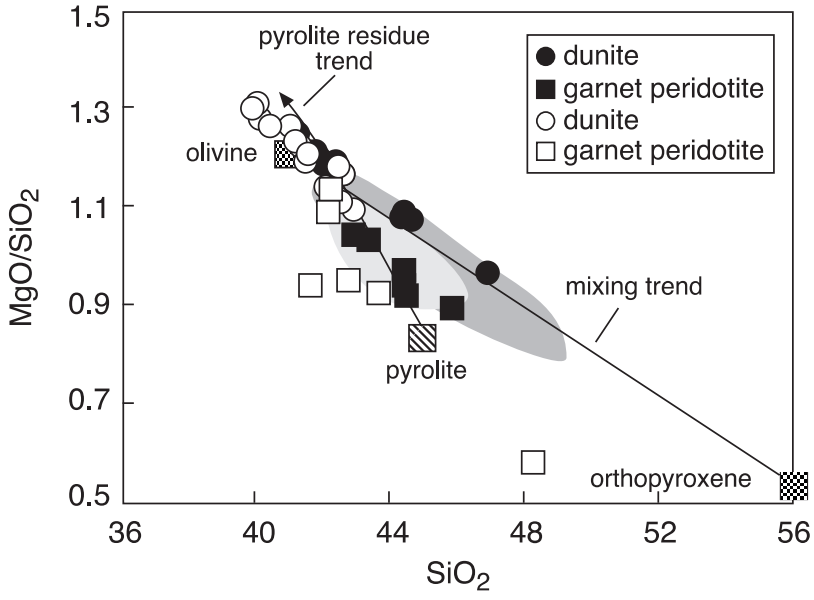

Fig. 13. Mg/SiO_2 vs SiO_2 (wt %) showing peridotites from Almklovdalen relative to the residue trend for pyrolite (KR4003), and to a mixing trend between olivine and opx (Walter, 1998). Published data taken from Eskola (1921), Mercy & O'Hara (1965*a*), Rost (personal communication, 1967), Finstadt & Heier (1972), Lappin (1974, 1975), Cordellier (1982) and Osland (1997). Dark grey area is the field for low-temperature garnet peridotites from the Kaapvaal and Siberia Cratons. Pale grey area is field for high-temperature garnet peridotites from the Kaapvaal and Siberia Cratons. All fields taken from Walter (1998).

rich in incompatible elements. Trace-element patterns in clinopyroxene and amphibole typically show strong negative anomalies in U, Zr, Hf and Ti, and enrichment in the LREE, Th, Sr and Y, characteristics that are indicative of metasomatism and show that the garnet-bearing rocks are not simply the product of melt depletion. Metasomatism in the lherzolites probably was volatile-rich, as indicated by the presence of amphibole in many of the samples.

The enrichment in LREE and LILE seen in the dunites indicates that they too are not simply melt residues and have probably been affected by at least one stage of the metasomatism that affected their enclosed garnet peridotites. This is supported by several similarities between the trace-element patterns for the two rock types including enrichment in the LREE, positive anomalies in Ba and Sr, and negative anomalies in U and Zr. The dunites contain rare amphibole and phlogopite, suggesting metasomatism by a volatile-rich fluid or melt as inferred for the garnet peridotites.

The compositional contrast between the dunites and the garnet peridotites poses the problem of how to reconcile the presence of small volumes of relatively fertile material within large bodies of extremely depleted material. The discrepancy in the pressure estimates for the garnet peridotites (~2 GPa) and dunites (3–7 GPa) at Almklovdalen derived from melt modelling (Fig. 13) suggests that the two rock types are not related by a simple melt-depletion process, and that their origins may not be validly inferred from the assumption that they both are residues. Given the spatial relationships between the two rock types, it appears highly unlikely that small volumes of garnet peridotite have undergone melt extraction at shallow depth, and then survived while the large volumes of surrounding dunite have been subjected to much higher degrees of melting at greater depth.

A more likely explanation is that the garnet peridotites represent metasomatic refertilization of the older dunites within the mantle, by processes similar to those that produced the high-temperature sheared peridotite xenoliths found in kimberlites. In this case, the garnet lherzolites are not simple residues. The shallow depth of 'melting' derived for the lherzolites thus is simply an artefact of the basic (and invalid) assumption (a single-stage melt-extraction process) involved in the modelling. It should be noted that this same artefact will invalidate attempts to model the origins of most xenolith suites.

The Western Gneiss Region garnet peridotites have previously been interpreted as representing cold, melt-depleted, buoyant lithospheric mantle based on their broad similarity to low-temperature coarse garnet peridotite xenoliths found in kimberlites (Carswell, 1968; Brueckner & Medaris, 1998). However, the bulk-rock and mineral compositions of the garnet peridotites are more closely analogous to the high-temperature sheared peridotite xenoliths found in kimberlites. High-temperature sheared peridotite xenoliths typically have higher FeO, Al_2O_3, CaO and NaO abundances, and

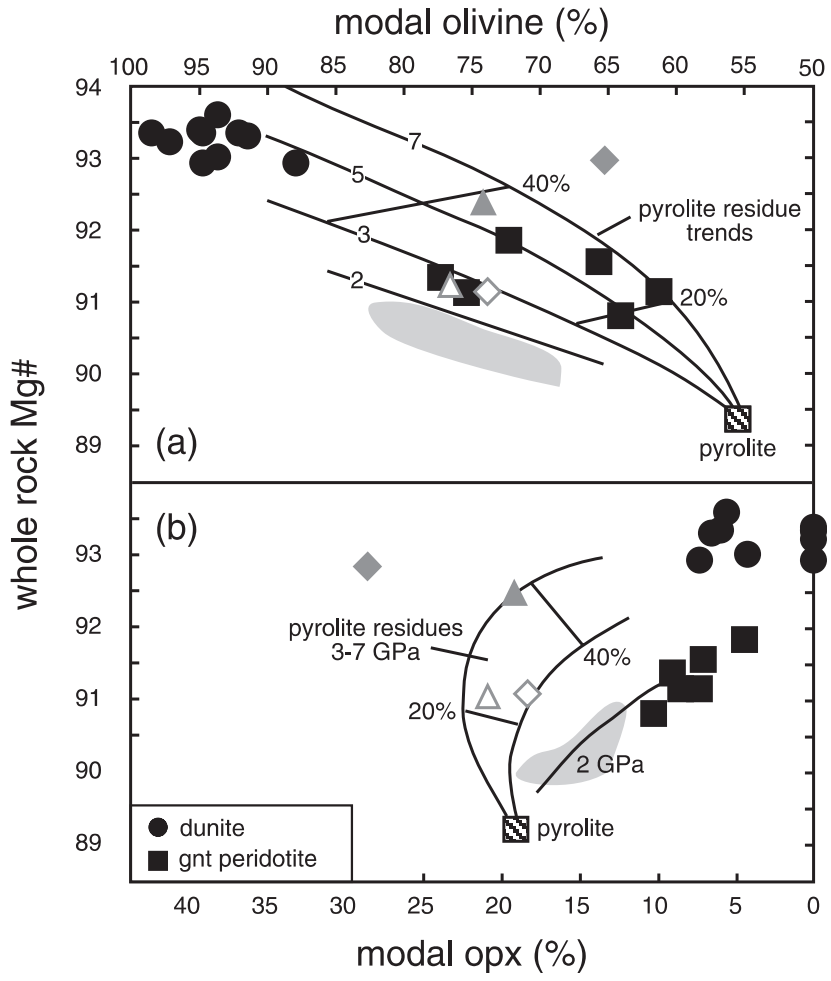

Fig. 14. Whole-rock Mg-number vs modal olivine (a) and modal opx (b) showing residue trends for melting of pyrolitic mantle [3–7 GPa, KR4003 (Walter, 1998); 2 GPa, KLB-1 (Hirose & Kushiro, 1993)]. Residue contours are labelled according to pressure (GPa) and per cent melting. After Walter (1998). Triangles represent average low-T (open) and high-T (filled) peridotites from Kaapvaal. Diamonds represent average low-T (open) and high-T (filled) peridotites from Siberia. Grey field is for oceanic peridotites. All averages and fields taken from Walter (1998).

higher Mg-number than their low-temperature counterparts (Griffin *et al.*, 1999*a*). The FeO contents of WGR garnet peridotites (Table 1) are not as high as the average FeO content seen in high-temperature peridotites (8·1 wt %), but are higher than the mean for cratonic low-temperature peridotites (6·4 wt %; Griffin *et al.*, 1998). Al_2O_3, CaO and Na_2O contents of the WGR peridotites are significantly higher than those of low-temperature peridotites and are also even higher than the mean values for high-temperature peridotites (Griffin *et al.*, 1999a). These compositions are more typical of metasomatized peridotite xenoliths from the kimberlites of the Kaapvaal Craton (Griffin *et al.*, 2003*b*) or highly fertile peridotites from Phanerozoic settings (e.g. Griffin *et al.*, 1999*a*). This similarity strongly suggests that the Almklovdalen garnet peridotites have been refertilized by melts rich in basaltic components, particularly Na, which occurs in abundances beyond even that for young fertile lherzolites.

If the analogy with high-T sheared peridotites is correct, the low temperatures reported for the WGR garnet peridotites (700–950°C: Jamtveit *et al.*, 1981; Medaris, 1984; Medaris & Carswell, 1990; Beyer, 2002) probably reflect equilibration to lower temperature over time, following formation as a result of high-T processes.

As discussed above, the garnets in the Almklovdalen peridotites have been classified as Class L9 and L10A garnets according to the CARP scheme of Griffin *et al.* (2002). These garnets are abundant in the shallow layers of both Archaean and Proterozoic mantle sections and are interpreted as refertilization of depleted harzburgites and lherzolites to depleted or metasomatized lherzolites (Griffin *et al.*, 2002). Mantle sections for Proterozoic terranes (i.e. Botswana, Yangtze and Birekte) considered by Griffin *et al.* (2002) all show a concentration of depleted or metasomatized garnets and some depleted ones towards the base of the sections; these grade upward into

dominantly fertile lherzolite and downward into lherzolites affected by melt-related metasomatism. The dominance of metasomatized garnets in Proterozoic mantle sections has led Griffin *et al.* (2002) to conclude that at least some Proterozoic lithosphere may represent strongly reworked Archaean lithospheric mantle. If this is the case for the garnet peridotite bodies from the WGR then it might be expected that Archaean isotopic signatures may be preserved in the reworked peridotite: this is discussed below.

A depleted precursor for the garnet peridotites

The occurrence of the garnet peridotites within the enclosing dunites, and the geochemical and mineralogical similarity of the garnet peridotites to high-temperature melt-metasomatized lherzolite xenoliths in kimberlites, suggests that the garnet peridotites represent pathways of percolating metasomatic agents in the mantle. From the composition of the garnet peridotites these are inferred to be mainly silicate melts rich in Fe, Ca, Al and Na but not K or Ti. These percolating fluids were also rich in incompatible trace elements such as the LREE, LILE (except Rb) and Th as evidenced by the variable enrichment of the peridotites in these elements. These melts may be similar to the magmas that formed the pyroxenites and eclogites that are closely associated with the garnet peridotites at Almklovdalen, and that show generally high Fe, Ca, Al and Na, but low K and Ti (see Fig. 4). This is supported by the very close similarity between the REE patterns for garnet peridotites and adjacent pyroxenites from the Lien locality in Almklovdalen (Brueckner & Medaris, 1998; Medaris & Brueckner, 2003). The peridotites have patterns that mirror, at lower REE concentrations, the patterns of the pyroxenites, suggesting that there is a strong link between the two rock types.

At Almklovdalen, the close spatial relationship between the garnet peridotite and associated mafic rocks, and the similarity in their whole-rock trace-element patterns, have been cited as evidence that at least one episode of metasomatism was caused by the intrusion of the pyroxenite melts (Brueckner & Medaris, 1998). Sm–Nd mineral dating from the Lien locality at Almklovdalen suggests that intrusion of the pyroxenites occurred at ~1·82 Ga (Brueckner & Medaris, 1998), although whether or not this intrusion event was the one that refertilized the dunites to form the garnet peridotites is not certain. It may be that intrusion of these melts occurred during the Sveconorwegian orogeny as indicated by the 1·04 Ga age determined for a pyroxenite from Raudkleivane (Jamtveit *et al.*, 1991). Sveconorwegian Lu–Hf ages have also been found in pyroxenites from the Sandvik peridotite body just north of Almklovdalen (Lapen *et al.*, 2005).

Further compelling evidence that the dunites are the depleted parent rocks to the garnet peridotites comes from the Re–Os isotopic system (Beyer *et al.*, 2004). Whole-rock Re–Os dating of the dunites has yielded Archaean Re-depletion model ages ($t_{RD} \approx 2{\cdot}7$–$3{\cdot}1$ Ga) suggesting that these rocks experienced an Archaean partial-melting event. This was an unexpected result, as there had been no previous evidence for an Archaean event in this part of the Baltic Shield. Re–Os dating of sulphide inclusions in silicates in the garnet peridotites yielded Proterozoic Re-depletion ages ($t_{RD} \approx 1{\cdot}7$ Ga) similar to the ages of the enclosing crustal rocks. However, Archaean Re–Os ages ($t_{RD} \approx 2{\cdot}9$–$3{\cdot}2$ Ga) have also been preserved in sulphides enclosed in olivine in the garnet peridotites. This observation strongly suggests a genetic link between the dunites and the garnet-bearing peridotites, and further supports the formation of the garnet peridotites by Proterozoic metasomatic refertilization of strongly depleted Archaean lithospheric mantle. These results are further supported by recent work on the Sandvik peridotite, which has found both Archaean and Proterozoic ages in garnet peridotites using the Lu–Hf and Sm–Nd isotopic systems (Lapen *et al.*, 2005).

Significance for understanding the evolution of lithospheric mantle

The process of refertilization of depleted Archaean mantle identified in this study may represent a common phenomenon occurring within the subcontinental lithospheric mantle as metasomatic fluids and melts continually percolate through this layer and modify its composition. This study reveals one consequence of such metasomatism and confirms that significant volumes of old depleted mantle may be metasomatically transformed as suggested by Bell *et al.* (2003), Coussaert *et al.* (2003) and Griffin *et al.* (2003*a*). Therefore, caution needs to be exercised in interpreting the significance of individual xenoliths. However, an understanding of rock-type relationships as revealed in this study, coupled with the use of Re–Os dating of mantle sulphides, can assist in unravelling the complex geochemical evolution of the mantle preserved in the xenolith record.

CONCLUSIONS

This study has demonstrated a strong case for a genetic link between the dunites and the garnet-bearing peridotites in the orogenic Western Gneiss terrane (Norway) by fluid percolation in the mantle. This outcome strongly indicates that some Proterozoic mantle garnet peridotites have formed by refertilization of strongly depleted Archaean lithospheric mantle as a result of mantle metasomatic processes (e.g. Griffin *et al.*, 1999*a*, 2003*a*;

Bell *et al.*, 2003; Coussaert *et al.*, 2003). Specific conclusions are listed below.

(1) The Almklovdalen dunites are residues after very high degrees of partial melting, probably at high pressures.

(2) The garnet peridotites are not simple melt residues. Their compositional similarity to high-temperature sheared peridotite xenoliths from kimberlites suggests that they formed by refertilization of a depleted precursor (in this case, the enclosing dunites).

(3) The close spatial relationship of the fertile garnet peridotites with veins and dykes of garnet pyroxenites and eclogites suggests that the garnet peridotite bodies formed in zones of melt percolation within the mantle, represented by the dunite. This is supported by parallel trace-element patterns for the garnet peridotites and adjacent pyroxenites.

(4) The refertilizing agent was a melt rich in Fe, Ca, Al, Na and LREE, and low in K and Ti, similar to the parent magmas of the garnet pyroxenites and eclogites that occur within the garnet peridotite bodies.

(5) Whole-rock Re–Os dating of the dunites (Beyer *et al.*, 2004) yielded Archaean model ages, indicating an Archaean depletion event. Sulphide Re–Os data for the garnet peridotites show a range from Archaean to Proterozoic model ages and provide strong evidence for a link between the two rock types by metasomatic transformation in Proterozoic time.

ACKNOWLEDGEMENTS

We thank Norman Pearson for numerous critical discussions and invaluable assistance with the analytical work. We are grateful to Suzy Elhlou for her assistance with LAM trace-element analysis, and to Carol Lawson for XRF work. This study was supported by the Australian Research Council, the GEMOC Key Centre and the Macquarie University Postgraduate Research fund. This is contribution 426 from the ARC National Key Centre for Geochemical Evolution and Metallogeny of Continents.

REFERENCES

Bell, D. R., Gregoire, M., Grove, T. L., Chatterjee, N. & Bowring, S. A. (2003). Silica and carbon deposition in the Kimberley peridotites. *Extended Abstracts of the 8th International Kimberlite Conference*, number FLA_0289.

Bernstein, S. & Brooks, C. K. (1999). Mantle xenoliths from Tertiary lavas and dykes at Ubekendt Ejland, West Greenland. *Geological Survey of Greenland Bulletin* **180**, 152–154.

Bernstein, S., Keleman, P. B. & Brooks, C. K. (1998). Depleted spinel harzburgite xenoliths in Tertiary dykes from East Greenland; restites from high degree melting. *Earth and Planetary Science Letters* **154**, 221–235.

Beyer, E. E. (2002). Evolution of the lithosphere beneath Tasmania and western Norway. Ph.D. thesis, Macquarie University, Sydney, 336 pp.

Beyer, E. E., Brueckner, H. K., Griffin, W. L., O'Reilly, S. Y. & Graham, S. (2004). Archean mantle fragments in Proterozoic crust, Western Gneiss Region, Norway. *Geology* **32**(7), 609–612.

Bodinier, J. L. (1988). Geochemistry and petrogenesis of the Lanzo peridotite body, Western Alps. *Tectonophysics* **149**, 67–88.

Bonatti, E., Ottonello, G. & Hamlyn, P. R. (1986). Peridotites from the island of Zabargad (St John), Red Sea: petrology and geochemistry. *Journal of Geophysical Research* **91**, 599–631.

Boyd, F. R. (1989). Compositional distinction between oceanic and cratonic lithosphere. *Earth and Planetary Science Letters* **96**, 15–26.

Boyd, F. R. (1997). Origins of peridotite xenoliths: major element considerations. In: Ranalli, G., Luchi, F. R., Ricci, C. A. & Tromsdorff, T. (eds) *High Pressure and High Temperature Research on Lithosphere and Mantle Materials*. University of Siena, pp. 89–106.

Boyd, F. R. & Canil, D. (1997). Peridotite xenoliths from the Slave Craton, Northwest Territories (abstract). *Seventh Annual Goldschmidt Conference, Houston*, pp. 34–35.

Boyd, F. R. & Finnerty, A. A. (1980). Conditions of origin of natural diamonds of peridotite affinity. *Journal of Geophysical Research* **85**(B12), 6911–6918.

Brueckner, H. K. (1977). A structural, stratigraphic and petrologic study of anorthosites, eclogites and ultramafic rocks and their country rocks, Tafjord area, Western South Norway. *Norges Geologiske Undersøkelse* **332**, 1–53.

Brueckner, H. K. & Medaris, L. G. (1998). A tale of two orogens: the contrasting *T–P–t* history and geochemical evolution of mantle in high- and ultrahigh-pressure metamorphic terranes of the Norwegian Caledonides and the Czech Variscides. *Schweizerische Mineralogische und Petrographische Mitteilungen* **78**, 293–307.

Brueckner, H. K. & Medaris, L. G. (2000). A general model for the intrusion and evolution of 'mantle' garnet peridotites in high-pressure and ultra-high-pressure metamorphic terranes. *Journal of Metamorphic Geology* **18**, 123–133.

Bryhni, I. (1966). Reconnaissance studies of gneisses, ultrabasites, eclogites and anorthosites in Outer Nordfjord, western Norway. *Norges Geologiske Undersökelse* **241**, 1–68.

Bryhni, I. & Green, D. H. (1970). On the occurrence of eclogites in western Norway. *Contributions to Mineralogy and Petrology* **26**, 12–19.

Bryhni, I., Bollingberg, H. J. & Graff, P. R. (1969). Eclogites in quartzo-felspathic gneisses of Nordfjord, west Norway. *Norsk Geologisk Tidsskrift* **49**, 193–225.

Carbno, G. B. & Canil, D. (2002). Mantle structure beneath the SW Slave Craton, Canada: constraints from garnet geochemistry in the Drybones Bay Kimberlite. *Journal of Petrology* **43**(1), 129–142.

Carswell, D. A. (1968*a*). Picritic magma–residual dunite relationships in garnet peridotite at Kalskaret near Tafjord, south Norway. *Contributions to Mineralogy and Petrology* **19**, 97–124.

Carswell, D. A. (1968*b*). Possible primary upper mantle peridotite in Norwegian basal gneiss. *Lithos* **1**, 322–355.

Carswell, D. A. (1974). Comparative equilibration temperatures and pressures of garnet lherzolites in Norwegian gneisses and in kimberlite. *Lithos* **7**, 113–121.

Carswell, D. A. (1981). Clarification of the petrology and occurrence of garnet lherzolites, garnet websterites and eclogite in the vicinity of Rødhaugen, Almklovdalen, West Norway. *Norsk Geologisk Tidsskrift* **61**, 249–260.

Carswell, D. A. (1986). The metamorphic evolution of Mg–Cr type Norwegian garnet peridotites. *Lithos* **19**, 279–297.

Carswell, D. A. & van Roermund, H. L. M. (2003). The occurrence and interpretation of garnet peridotite bodies in the Western Gneiss

Region. In: Carswell, D. A. (ed.) *Guidebook to the Post-Selje Eclogite Field Symposium Field Excursion*. Trondheim: Norges Geologiske Undersøkelse.

Carswell, D. A., Cuthbert, S. J. & Krogh Ravna, E. J. (1999). Ultrahigh-pressure metamorphism in the Western Gneiss Region of the Norwegian Caledonides. *International Geology Review* **41**, 955–966.

Coleman, R. G. & Wang, X. (1995). Overview of the geology and tectonics of UHPM. In: Coleman, R. G. & Wang, X. (eds) *Ultrahigh Pressure Metamorphism*. Cambridge: Cambridge University Press, pp. 1–33.

Cordellier, F. M., Boudier, F. & Boullier, A. M. (1981). Structural study of the Almklovdalen peridotite massif (southern Norway). *Tectonophysics* **77**, 257–281.

Coussaert, N., Gregoire, M., Mercier, J. C., Bell, D., Demaiffe, D., le Roex, A. & Andre, L. (2003). The origin of clinopyroxene in cratonic mantle. *Extended Abstracts of the 8th International Kimberlite Converence*, number FLA_0383.

Cuthbert, S. J., Harvey, M. A. & Carswell, D. A. (1983). A tectonic model for the metamorphic evolution of the Basal Gneiss Complex, Norwegian Caledonides. *Journal of Metamorphic Geology* **1**, 63–90.

Cuthbert, S. J., Carswell, D. A., Krogh-Ravna, E. J. & Wain, A. (2000). Eclogites and eclogites in the Western Gneiss Region, Norwegian Caledonides. *Lithos* **52**, 165–195.

Ernst, W. G., Liou, J. G. & Coleman, R. G. (1995). Comparative petrotectonic study of five Eurasian ultrahigh-pressure metamorphic complexes. *International Geology Review* **37**, 191–211.

Eskola, P. (1921). On the eclogites of Norway. *Skrifter Utgitt av det Norske Videnskaps-selsk. Christiana, Matematisk-Naturvidenskapelig Klasse* **18**, 1–118.

Finstadt, K. G. & Heier, K. S. (1972). The distribution of some elements between the metal and silicate phases obtained in a smelting reduction process of dunite from Almklovdalen, west Norway. *Earth and Planetary Science Letters* **16**, 209–212.

Godard, M., Jousselin, D. & Bodinier, J.-L. (2000). Relationships between geochemistry and structure beneath a palaeo-spreading centre: a study of the mantle section in the Oman ophiolite. *Earth and Planetary Science Letters* **180**, 133–148.

Green, D. H. & Mysen, B. O. (1972). Genetic relationship between eclogite and hornblende + plagioclase pegmatite in western Norway. *Lithos* **5**, 147–161.

Griffin, W. L. & Mørk, M. B. E. (1981). Eclogites and basal gneisses in western Norway. *Uppsala Caledonide Symposium. Mineralogisk–Geologisk Museum, Excursion Guide B1*, 88 pp.

Griffin, W. L. & Qvale, H. (1985). Superferrian eclogites and the crustal origin of garnet peridotites, Almklovdalen, Norway. In: Gee, D. G. & Sturt, B. A. (eds) *The Caledonide Orogen—Scandinavia and Related Areas*. Chichester: John Wiley, pp. 803–812.

Griffin, W. L. & Råheim, A. (1973). Convergent metamorphism of eclogites and dolerites, Kristiansund area, Norway. *Lithos* **6**, 21–40.

Griffin, W. L., Austrheim, H., Brastad, K., Bryhni, I., Krill, A. G., Krogh, H. K., Mørk, M. B. E., Qvale, H. & Tørudbakken, B. (1985). High-pressure metamorphism in the Scandinavian Caledonides. In: Gee, D. G. & Sturt, B. A. (eds) *The Caledonide Orogen—Scandinavia and Related Areas*. Chichester: John Wiley, pp. 783–801.

Griffin, W. L., Cousens, D. R., Ryan, C. G., Sie, S. H. & Suter, G. F. (1989*a*). Ni in chrome pyrope garnets: a new geothermometer. *Contributions to Mineralogy and Petrology* **103**, 199–202.

Griffin, W. L., Smith, D., Boyd, F. R., Cousens, D. R., Ryan, C. G., Sie, S. H. & Suter, G. F. (1989*b*). Trace element zoning in garnets from sheared mantle xenoliths. *Geochimica et Cosmochimica Acta* **53**, 561–567.

Griffin, W. L., O'Reilly, S. Y., Ryan, C. G., Gaul, O. & Ionov, D. A. (1998). Secular variation in the composition of subcontinental lithospheric mantle: geophysical and geodynamic implications. In: Braun, J., Dooley, J. C., Goleby, B. R., van der Hilst, R. D. & Klootwijk, C. T. (eds) *Structure and Evolution of the Australian Continent*. Washington, DC: American Geophysical Union, pp. 1–26.

Griffin, W. L., O'Reilly, S. Y. & Ryan, C. G. (1999*a*). The composition and origin of subcontinental lithospheric mantle. In: Fei, Y., Bertka, C. M. & Mysen, B. O. (eds) *Mantle Petrology: Field Observations and High Pressure Experimentation: a Tribute to Francis F. (Joe) Boyd*. Houston, TX: Geochemical Society, pp. 13–45.

Griffin, W. L., Shee, S. R., Ryan, C. G., Win, T. T. & Wyatt, B. A. (1999*b*). Harzburgite to lherzolite and back again: metasomatic processes in ultramafic xenoliths from the Wesselton kimberlite, Kimberley, South Africa. *Contributions to Mineralogy and Petrology* **134**, 232–250.

Griffin, W. L., Ryan, C. G., Kaminsky, F. V., O'Reilly, S. Y., Natapov, L. M., Win, T. T., Kinny, P. D. & Ilupin, I. P. (1999*c*). The Siberian lithosphere traverse: mantle terranes and the assembly of the Siberian Craton. *Tectonophysics* **310**, 1–35.

Griffin, W. L., Fisher, N. I., Friedman, J. H., O'Reilly, S. Y. & Ryan, C. G. (2002). Cr-pyrope garnets in the lithospheric mantle. II. Compositional populations and their distribution in time and space. *Geochemistry, Geophysics, Geosystems* **3**(12), 1073, doi:10.1029/2002GC000298.

Griffin, W. L., O'Reilly, S. Y., Abe, N., Aulbach, S., Davies, R. M., Pearson, N. J., Doyle, B. J. & Kivi, K. (2003*a*). The origin and evolution of Archean lithospheric mantle. *Precambrian Research* **127**, 19–41.

Griffin, W. L., O'Reilly, S. Y., Natapov, L. M. & Ryan, C. G. (2003*b*). The evolution of lithospheric mantle beneath the Kalahari Craton and its margins. *Lithos* **71**, 215–242.

Grønlie, G. & Rost, F. (1974). Gravity investigation and geological interpretation of the ultramafite complex of Åheim, Sunnmøre, western Norway. *Norsk Geologisk Tidsskrift* **54**, 367–373.

Harte, B. (1983). Mantle processes and processes—the kimberlite sample. In: Hawkesworth, C. J. & Norry, M. J. (eds) *Continental Basalts and Mantle Xenoliths*. Nantwich: Shiva, pp. 46–91.

Hirose, K. & Kushiro, I. (1993). Partial melting of dry peridotites at high pressures: determination of compositions of melts segregated from peridotite using aggregates of diamond. *Earth and Planetary Science Letters* **114**, 477–489.

Hoal, K. E. O., Hoal, B. G., Erlank, A. J. & Shimizu, N. (1994). Metasomatism of the mantle lithosphere recorded by rare earth elements in garnets. *Earth and Planetary Science Letters* **126**, 303–313.

Jamtveit, B., Carswell, D. A. & Mearns, E. W. (1991). Chronology of the high-pressure metamorphism of Norwegian garnet peridotites/pyroxenites. *Journal of Metamorphic Geology* **9**, 125–139.

Krogh, E. J. & Carswell, D. A. (1995). HP and UHP eclogites and garnet peridotites in the Scandinavian Caledonides. In: Coleman, R. G. & Wang, X. (eds) *Ultrahigh Pressure Metamorphism*. Cambridge: Cambridge University Press, pp. 244–299.

Lapen, T. J., Medaris, L. G., Johnson, C. M. & Beard, B. L. (2005). Archean to Middle Proterozoic evolution of Baltica subcontinental lithosphere: evidence from combined Sm–Nd and Lu–Hf isotope analyses of the Sandvik ultramafic body, Norway. *Contributions to Mineralogy and Petrology* **150**, 131–145.

Lappin, M. A. (1966). The field relationships of basic and ultrabasic masses in the basal gneiss complex of Stadlandet and Almklovdalen, Nordfjord, southwestern Norway. *Norsk Geologisk Tidsskrift* **46**(4), 439–496.

Lappin, M. A. (1973). An unusual clinopyroxene with complex lamellar intergrowths from an eclogite in the Sunndal–Grubse ultramafic mass, Almklovdalen, Nordfjord, Norway. *Mineralogical Magazine* **39**, 313–320.

Lappin, M. A. (1974). Eclogites from the Sunndal–Grubse ultramafic mass, Almklovdalen, Norway and the *T–P* history of the Almklovdalen masses. *Journal of Petrology* **15**(3), 567–601.

Lappin, M. A. & Smith, D. C. (1978). Mantle-equilibrated orthopyroxene eclogite pods from the basal gneisses in the Selje district, western Norway. *Journal of Petrology* **19**, 530–584.

Lee, C.-T. & Rudnick, R. (1999). Compositionally stratified cratonic lithosphere: petrology and geochemistry of peridotite xenoliths from the Labait volcano, Tanzania. In: Gurney, J. J., Gurney, J. L., Pascoe, M. D. & Richardson, S. H. (eds) *Proceedings of Seventh International Kimberlite Conference*. Cape Town: Red Roof Design, pp. 503–521.

McDonough, W. F. & Sun, S.-s. (1995). The composition of the Earth. *Chemical Geology* **120**, 223–253.

Mearns, E. E. (1986). Sm–Nd ages for Norwegian garnet peridotite. *Lithos* **19**, 269–278.

Medaris, L. G. (1980). Convergent metamorphism of eclogite and garnet-bearing ultramafic rocks at Lien, West Norway. *Nature* **283**, 470–472.

Medaris, L. G. (1984). A geothermobarometric investigation of garnet peridotites in the Western Gneiss Region of Norway. *Contributions to Mineralogy and Petrology* **87**, 72–86.

Medaris, L. G. (1999). Garnet peridotites in Eurasian high-pressure and ultrahigh-pressure terranes: a diversity of origins and thermal histories. *International Geology Review* **41**, 799–815.

Medaris, L. G. & Brueckner, H. K. (2003). Excursion to the Almklovdalen peridotite. In: Carswell, D. A. (ed.) *Guidebook to the Field Excursions in the Nordfjord–Stadlandet–Almklovdalen Area*. Trondheim: Norges Geologiske Undersøkelse.

Medaris, L. G. & Carswell, D. A. (1990). The petrogenesis of Mg–Cr garnet peridotites in European metamorphic belts. In: Carswell, D. A. (ed.) *Eclogite Facies Rocks*. New York: Chapman and Hall, pp. 260–290.

Mercy, E. L. P. & O'Hara, M. J. (1965*a*). Chemistry of some garnet-bearing rocks from the south Norwegian peridotites. *Norsk Geologisk Tidsskrift* **45**, 323–332.

Mercy, E. L. P. & O'Hara, M. J. (1965*b*). Olivines and orthopyroxenes from garnetiferous peridotites and related rocks. *Norsk Geologisk Tidsskrift* **45**, 457–461.

Nixon, P. H. (1987). Kimberlitic xenoliths and their cratonic setting. In: Nixon, P. H. (ed.) *Mantle Xenoliths*. New York: John Wiley, pp. 215–239.

Norman, M. D., Pearson, N. J., Sharma, A. & Griffin, W. L. (1996). Quantitative analysis of trace elements in geological materials by laser ablation ICPMS: instrumental operating conditions and calibration values of NIST glasses. *Geostandards Newsletter* **20**(2), 247–261.

O'Hara, M. J. (1967). *Mineral Facies in Ultrabasic Rocks. Ultramafic and Related Rocks*. New York: John Wiley, pp. 7–18.

O'Hara, M. J. & Mercy, E. L. P. (1963). Petrology and petrogenesis of some garnetiferous peridotites. *Transactions of the Royal Society of Edinburgh* **65**, 251–314.

O'Hara, M. J., Richardson, S. W. & Wilson, G. (1971). Garnet peridotite stability and occurrence in crust and mantle. *Contributions to Mineralogy and Petrology* **32**, 48–68.

O'Reilly, S. Y. & Griffin, W. L. (1988). Mantle metasomatism beneath western Victoria, Australia: I. Metasomatic processes in Cr-diopside lherzolites. *Geochimica et Cosmochimica Acta* **52**, 433–447.

O'Reilly, S. Y., Griffin, W. L., Poudjom Djomani, Y. H. & Morgan, P. (2001). Are lithospheres forever? Tracking changes in subcontinental lithospheric mantle through time. *GSA Today* **11**(4), 4–10.

Osland, R. (1997). Modelling of variations in Norwegian olivine deposits, causes of variation and estimation of key quality factors. Doktor Ingeniør thesis, Norwegian University of Science and Technology, 189 pp.

Rudnick, R. L., McDonough, W. F. & Chappell, B. W. (1993). Carbonatite metasomatism in the northern Tanzanian mantle: petrographic and geochemical characteristics. *Earth and Planetary Science Letters* **114**, 463–475.

Scott Smith, B. H. (1987). Greenland. In: Nixon, P. H. (ed.) *Mantle Xenoliths*. New York: John Wiley, pp. 23–32.

Shervais, J. W. & Mukasa, S. B. (1991). The Balmuccia orogenic lherzolite massif, Italy. *Journal of Petrology, Special Lherzolites Issue* 155–174.

Shimizu, N. (1975). Rare earth elements in garnets and clinopyroxenes from garnet lherzolite nodules in kimberlites. *Earth and Planetary Science Letters* **25**, 26–32.

Shimizu, N. & Richardson, S. H. (1987). Trace element abundance patterns of garnet inclusions in peridotite-suite diamonds. *Geochimica et Cosmochimica Acta* **51**, 755–758.

Smith, D., Griffin, W. L. & Ryan, C. G. (1993). Compositional evolution of high-temperature sheared lherzolite PHN1611. *Geochimica et Cosmochimica Acta* **57**, 605–613.

Stachel, T., Viljoen, K. S., Brey, G. & Harris, J. W. (1998). Metasomatic processes in lherzolitic and harzburgitic domains of diamondiferous lithospheric mantle: REE in garnets from xenoliths and inclusions in diamonds. *Earth and Planetary Science Letters* **159**, 1–12.

Takahashi, E. (1986). Melting of a dry peridotite KLB-1 up to 14 GPa: implications on the origin of peridotitic upper mantle. *Journal of Geophysical Research* **91**, 9367–9382.

van Achterbergh, E., Griffin, W. L. & Stiefenhofer, J. (2001). Metasomatism in mantle xenoliths from the Letlhakane kimberlites: estimation of element fluxes. *Contributions to Mineralogy and Petrology* **141**, 397–414.

Walter, M. J. (1998). Melting of garnet peridotite and the origin of komatiite and depleted lithosphere. *Journal of Petrology* **39**(1), 29–60.

Xu, X., O'Reilly, S. Y., Griffin, W. L. & Zhou, X. (2000). Genesis of young lithospheric mantle in southeastern China: a LAM-ICPMS trace element study. *Journal of Petrology* **40**, 111–148.

Yao, S. (1999). Chemical composition of chromites from ultramafic rocks: application to mineral exploration and petrogenesis. Ph.D. thesis, Macquarie University, Sydney, 191 pp.